1 OF 1

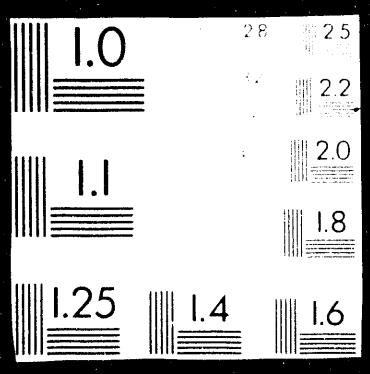

LAUR-92-310

GEOLOGIC MAPPING OF THE SEMIPALATINSK REGION, EASTERN KAZAKSTAN, USING LANDSAT THEMATIC MAPPER AND SPOT PANCHROMATIC DATA

SEP 14 1992
OSTI

by

Philip A. Davis, USGS Flagstaff and
G. Lennis Berlin, Northern Arizona University

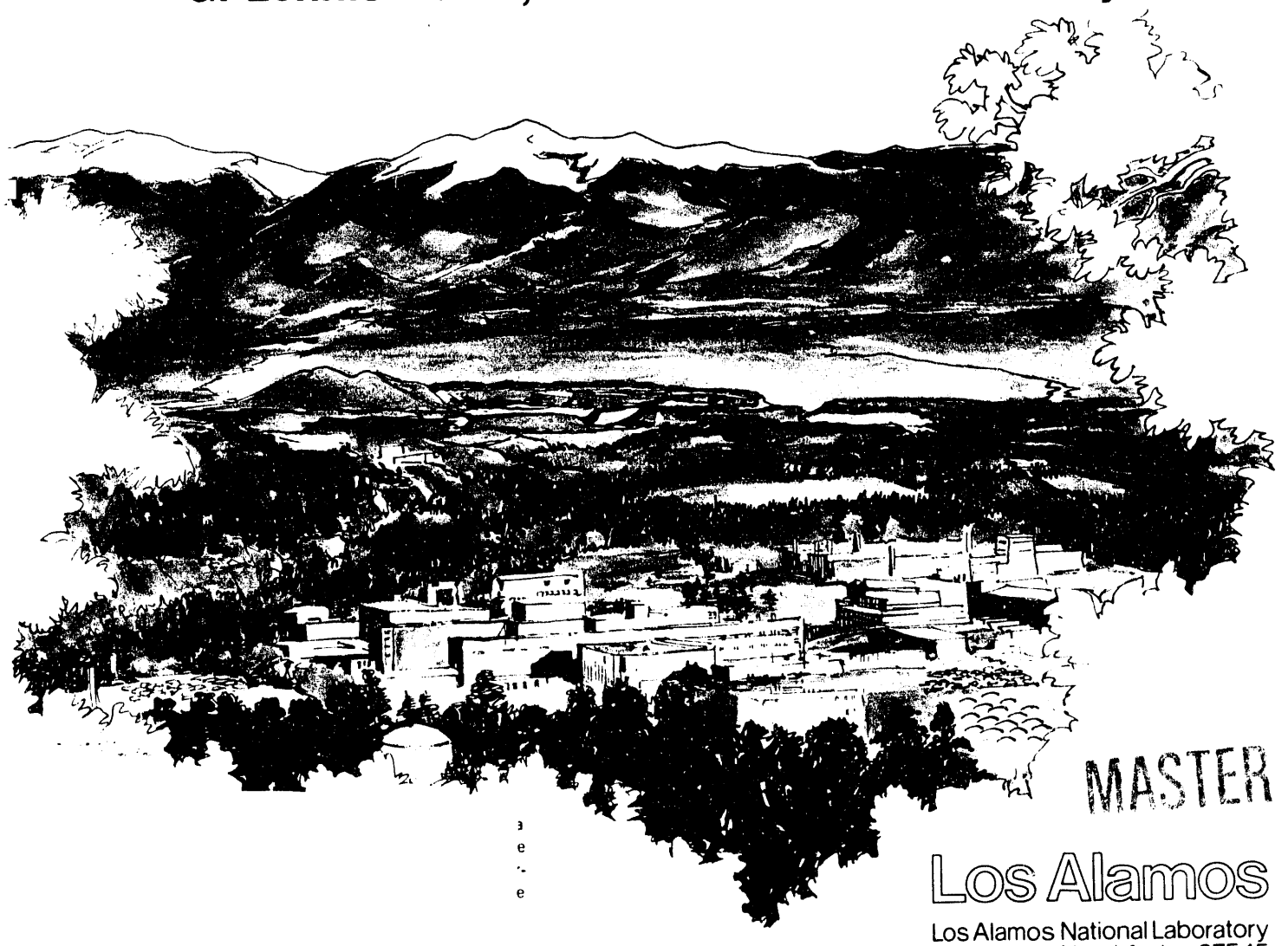

MASTER

Los Alamos
Los Alamos National Laboratory
Los Alamos, New Mexico 87545

DISTRIBUTION OF THIS DOCUMENT IS UNLIMITED

DISCLAIMER

This report was prepared as an account of work sponsored by an agency of the United States Government. Neither the United States Government nor any agency thereof, nor any of their employees, makes any warranty, express or implied, or assumes any legal liability or responsibility for the accuracy, completeness, or usefulness of any information, apparatus, product, or process disclosed, or represents that its use would not infringe privately owned rights. Reference herein to any specific commercial product, process, or service by trade name, trademark, manufacturer, or otherwise does not necessarily constitute or imply its endorsement, recommendation, or favoring by the United States Government or any agency thereof. The views and opinions of authors expressed herein do not necessarily state or reflect those of the United States Government or any agency thereof.

INTRODUCTION

This geologic reconnaissance study centers on a 90 by 140 km area about 100 km southwest of Semipalatinsk near the east border of the Kazakstan Republic of the U.S.S.R. (Figures 1 and 2). Semipalatinsk, a regional center for grain growing, and several other cities along the Irtysh River were originally established as fortified outposts by the Russians during the 18th and 19th centuries to contain the indigenous, nomadic Kazak herdsmen. The Kazakstan region remained largely undeveloped until after the 1917 Russian Revolution, when exploration geologists began discovering many large mineral deposits. Today, known resources include coal, copper, iron ore, lead, zinc, and barite; most of these are of national significance. These vast mineral resources have prompted development of many metallurgical and chemical industries in the republic.

Despite the extensive exploration for mineral resources in this region, published geologic maps (Nalivkin, 1960; Esenov, 1971; Borovikov, 1972) are all at scales of 1:1,100,000 or smaller, and there are no detailed descriptions of the geology around Semipalatinsk in the open literature. Our preliminary examination of commercial remote-sensing data indicated that the lithology and structure of this area are extremely varied and complex at all scales--much more so than that portrayed on the published geologic maps. Therefore, the main objective of this study was to use commercially available remotely sensed data for the area and remotely sensed data obtained for analog study sites, as well as the sparse, sketchy information in the published literature, to better define and map the geologic units (Sheet 1), structure (Sheet 2), and drainage features (Sheet 3) of this area.

PHYSICAL SETTING

The physiography of the Semipalatinsk area looks like the result of Appalachian style tectonics modified by weathering of the U.S. Southwest. The perennial Irtysh River, which is located just north of the study area (Figure 2), approximates the boundary between the Kazakstan steppe to the south and the western Siberian lowlands (tundra) to the north. The Kazakstan steppe has also been referred to as the Kirgiz steppe and the Sary Arka (Nalivkin, 1973). The steppe is characterized by relatively flat watersheds and wide river valleys (Nalivkin, 1973).

The climate of the study area is semi-arid or middle-latitude steppe (Köppen Classification=BSk), with a mean annual precipitation:potential-evapotranspiration ratio of 0.20 to 0.50 (UNESCO, 1977). This climate classification is the same as those of Reno (Nevada), Ankara (Turkey), and Tehran (Iran). The temperature regime (Table 1) is characterized by hot summers, cold winters, and marked diurnal variations during most of the year. Annual precipitation is less than 300 mm, much of which falls in two seasons -- one in summer, the other in late fall and early winter (Table 1). The dry climate is reflected in the area's many

playas and intermittent streams, paucity of natural vegetation, and dominance of irrigated agriculture (green and yellow rectangular areas in Figure 3). Consequently, most of the cities, towns, and arable land in the study area are located along the Shagan River that flows northward through the center of the study area to the Irtysh River. Intermittent surface runoff mostly follows consequent, obsequent, and subsequent patterns. Much of the study area is a flat plain of gentle relief, at an elevation of about 240-380 m. This topography is broken by rolling hills (called "sopkas") and ridges rising above 565 m; the highest elevation within the study area is 1,075 m on Degelan Mountain (Figures 3 and 4).

Table 1. Average Temperature/Precipitation Regime at Semipalatinsk (latitude 50° 24' N., elevation 216.2 m)

Month	Temperature (°C)	Rainfall (mm)
January	-17	20.3
February	-16	12.7
March	-13	12.7
April	4	15.2
May	15	25.4
June	20	43.2
July	22	30.5
August	19	25.4
September	13	15.2
October	5	28.0
November	-6	28.0
December	-13	22.9
Total for year		279.5

Adapted from Rumney (1968).

Within the Kazakstan region are several important coal and copper mining operations (Khain, 1985). Coal is mined at Karaganda and Pavlodar (Figure 2), while copper is mined at Dzhezkazgan (northwest of the area shown on Figure 2). Power for mining operations is provided by hydroelectric stations on the Irtysh River east of Semipalatinsk (Nalivkin, 1973).

GEOLOGIC SETTING

The very complex geologic and structural setting of the Semipalatinsk area is the result of a prolonged history of extension and compression involving the Siberian and Kazakstan continental plates and intervening island arcs (Zonenshain et al., 1990). In this region, the boundary between these two continental plates is approximated by the Irtysh River (Figure 2). Given its tectonic history, it is not surprising that the Semipalatinsk area has many geologic attributes of the thrust-faulted Appalachian fold belt. Unlike the Appalachians, however, the Semipalatinsk area has an erosional and weathering regime like that of the southwestern United States: rocks in the Semipalatinsk area have been exposed to semi-arid to arid conditions for most, if not all, of the Quaternary Period.

The following discussion is a synopsis of the geologic events that have occurred within this region as hypothesized by Soviet geologists (Nalivkin, 1960, 1973; Rotarash et al., 1980, 1982; Rotarash and Gredyushko, 1980; Rotarash and Trubnikov, 1983; Zonenshain et al., 1990). The region has undergone several episodes of tectonism involving both folding and faulting, which have been grouped into the Caledonian and Hercynian Ages (Nalivkin, 1960). Some geologists assign early and late subdivisions to each of these ages (Zonenshain et al., 1990). The Caledonian Age (early Paleozoic) involved mostly accretion of numerous blocks (Zonenshain et al., 1990) and is represented by various degrees of faulting, folding, and metamorphism (Nalivkin, 1960). In Hercynian (late Paleozoic) time, the Siberian and Kazakstan continental plates collided repeatedly (Zonenshain et al., 1990); the age is represented by volcanic materials, granites, and well-folded sedimentary rocks (Nalivkin, 1960).

Most folds of Caledonian time in Europe and Asia are extended northeastward, whereas folds of Hercynian time are extended northwestward (Nalivkin, 1960). The folds and faults in the Semipalatinsk area trend mostly northwest, and average dips of the strata are 40° to 50° to the southwest (e.g., Rotarash et al., 1980).

The intrusives in this region are associated with specific phases of folding and thus can be separated into different generations (Nalivkin, 1960). During the Caledonian tectonism, basic volcanism was widespread and ophiolite belts formed along with spilites and pillow lavas (which indicate submarine eruptions) and tuffs. Hercynian intrusives were not affected by folding and therefore have rounded outlines, no connection with tectonic structures, and uniform composition. Such late intrusives break through upper Paleozoic coal-bearing strata near Semipalatinsk.

In terms of plate tectonics, the first collision in this region for which there is evidence occurred in the Late Cambrian (referred to as the "Salairide Orogeny"), which formed island arcs between the continental plates (Zonenshain et al., 1990). The orogeny resulted in granitic intrusions and folding and metamorphism of limestone beds (Nalivkin, 1973). During the Early to Middle Ordovician there was back-arc spreading (Zonenshain et al., 1990) with

accumulations of limestone, greywacke, and conglomerate (Nalivkin, 1973). In the Silurian and Devonian, the island arcs collided again (Zonenshain et al., 1990), forming alternations of continental, marine, lagoonal, and volcanic deposits (Nalivkin, 1973). In Middle to Late Devonian time, the Kazakstan and Siberian continental plates collided and produced subduction zones (Zonenshain et al., 1990), which are represented in the study area mostly by red sandstones and shales.

Throughout Carboniferous time, the Kazakstan and Siberian plates continued to collide (Zonenshain et al., 1990); most deposits were continental sandstones, shales, and coal-bearing sequences (Nalivkin, 1973). With continued continental collision and uplift, deposits changed to mostly continental red sandstones and coal (Nalivkin, 1973). The main collision during middle Carboniferous time produced nappe structures (Zonenshain et al., 1990). Granitic batholiths formed during late Carboniferous and Early Permian collisional phases (Zonenshain et al., 1990). Permian deposits range from bituminous shales and coals to sandstones, clays, and marls as the environment changed from marine to continental (Nalivkin, 1973; Zonenshain et al., 1990). This last compressional period produced metamorphism, nappe structures, and dextral or right-lateral faults. Also during the Permian, several fold and fault zones formed. From west (within the study area) to east, some of the nearby zones are the Chingiz, Zharma, Irtysh-Zaysan, and Kalba-Narym (Zonenshain et al., 1990). The Chingiz system is a major strike-slip fault (Zonenshain et al., 1990).

Sands, clays, and gravels formed by continental erosion during Tertiary and Quaternary time. Quaternary sediments also include river and lake sands and clays. The alluvial and fluvial sediments may range between 30 to 80 m in thickness (e.g., near Pavlodar) and 1200 to 1500 m in thickness (e.g., within the basin surrounding Lake Zaysan, Figure 2).

DIGITAL ANALYSIS OF REMOTELY SENSED DATA

The Semipalatinsk study area is contained within Landsat-4 Thematic Mapper (TM) scene 42575-05110 (Figures 3 and 4), acquired 03 August 1989 with a sun elevation angle of 52.6° and a sun azimuth of 139°. In addition to this Landsat multispectral data, we also used a Satellite Pour l' Observation de la Terre (SPOT) panchromatic scene of the west half of the study area; this scene (Figure 5) was acquired 12 June 1988 with a sun elevation angle of 62.7°, a sun azimuth of 165.9°, and a spacecraft incidence (viewing) angle of 26.5°. Although the two databases are different, both provide critical information for our analyses. Landsat TM multispectral data (30-m spatial resolution) provide spectral reflectance values within six wavelength bands (from the blue to the middle infrared wavelengths); the values are indicative of mineralogic and elemental compositions. The SPOT panchromatic data (10-m spatial resolution) allow improved interpretation of spatial relations. In addition, the SPOT data allow improved geologic and structural analyses because their oblique viewing geometry, combined with the near-vertical viewing of the Landsat sensor, provides a stereoimage pair for three-dimensional analysis.

It is necessary to determine and remove the amount of atmospheric scattering (also referred to as haze) within each of the six Landsat nonthermal bands before performing image-processing algorithms. In semi-arid and arid regions, determination of haze is usually difficult because of the scarcity of features that allow direct measurement of haze, such as a relatively large area of either deep water or true shadow (the latter requires relief or thick, isolated clouds). Although relief is minimal in the study area, there are several areas of deep water that allowed easy determination of the haze value for each TM band. The resultant set of TM-band haze values is consistent with theoretical values at the TM nonthermal wavelength bands for "clear" (λ^{-2}) atmospheric conditions as defined by Chavez (1988). The haze value for each nonthermal band was subtracted from the digital data for each respective TM band before beginning the digital analysis and processing.

Statistical-analysis methods were used on the six nonthermal TM bands to determine which combinations of three bands and of three band ratios provide optimum information content; all combinations of three-band and three band-ratio data (Chavez et al., 1982; Sheffield, 1985; Crippen, 1989) were considered. The logarithms of the band-ratio values were used in the band-ratio analysis, because the logarithm of a ratio does not change when the denominator and numerator are reversed. Results obtained by the Sheffield and Crippen methods indicate that the best three-band combinations include TM bands 1, 4, and 5 (or 7) and TM bands 1, 5, and 7. These same statistical results have been obtained in several other remote-sensing studies of semi-arid and arid regions (Sheffield, 1985; Davis et al., 1987; Crippen, 1989; Davis and Berlin, 1989); visual analysis of these three-band combinations verified the statistical results. We selected the band color composite (BCC) using TM bands 1, 4, and 7 for our geologic analysis (Figures 3 and 6).

The statistical analyses on the band ratios produced quite unusual results for arid to semi-arid environments. Most of the ratios in the top-ranked band-ratio combinations involved visible-wavelength bands. Visual examination of the indicated band-ratio color composites showed them to be inferior to other band-ratio combinations. The band-ratio statistical results for Semipalatinsk do not correspond to statistical and visual analyses of band-ratio combinations for other arid and semi-arid study areas, which have shown that the band-ratio combinations that provide the best geologic-unit discrimination include the band 5/band 4 (or 3) and band 7/band 5 ratios and the band 3 (or 4)/band 1 ratio (Davis et al., 1987; Crippen, 1989; Davis and Berlin, 1989). The areas examined in these studies have little vegetation, whereas the Semipalatinsk area has a considerable number of cultivated fields (yellow and green rectangles in Figure 6). Our attempts to define areas for statistical analysis that appear to have diverse geology but little vegetation produced similar results, as noted above. As a result, the band-ratio images proved to be of little use in our mapping efforts and are not shown in this report.

We also performed two analyses that usually result in image products that provide very good geologic discrimination in arid to semi-arid regions: decorrelation stretching (Gillespie et al., 1986) and principal-component (PC) analysis. We applied a decorrelation stretch to TM bands 1, 4, and 7 (DSC, Figure 7). We also applied PC analysis to TM bands 1, 4, and 7, as

well as to all six nonthermal TM bands. We produced a color-composite image using the three-component images from the first PC analysis, and we produced several composite images using various combinations of the six-component images from a second PC analysis. Visual examination of all the PC color-composite images showed that the best geologic discrimination was achieved by using PC1, PC4, and PC5 from the second PC analysis (PCC, Figure 8). Examination of the DSC and PCC images shows that the DSC image provides more lithologic information than the PCC image. The PCC image was used mostly in the analysis of drainage features.

One of the most useful image products that we found for interpretation of surface morphology was the PC1 data that resulted from the PC analysis of all six nonthermal TM bands. The first principal-component image in a PC analysis contains most of the variance of the data that are used in the PC analysis. A significant part of the variance in TM band data is produced by solar illumination on the topography (i.e., bright and dark slopes). Therefore, PC1 data contain most of the topographic information from the TM-band data. We enhanced the morphologic detail in this image by applying a digital high-pass filter with a spatial dimension of 101 by 101 picture elements or pixels (Figure 9). This image was used in our analysis of structural geology and drainage features.

ANALYSIS OF SURFACE GEOLOGY

For inaccessible areas where little is known about the geology, such as this study area, the most accurate identification of geologic materials is achieved by using mostly the BCC (Figure 6), DSC (Figure 7), SPOT panchromatic (Figure 5), and to a lesser extent the natural-color (Figure 4) image products. With remotely sensed data, geologic materials are identified on the basis of material brightness, TM-band reflectance, morphology (i.e., relief, jointing, weathering characteristics, outcrop and erosional patterns), and spatial geologic relations. These four image products directly provide this information. PC analysis or band ratioing usually enhances discrimination between geologic materials in arid and semi-arid regions. However, these latter two image products cannot be used to identify geologic materials without a priori knowledge of the geology.

The color assignments and wavelengths of the three TM bands used in the BCC and DSC images (Figures 6 and 7, respectively) depict mineral groups and rock types as different colors. For arid and semi-arid regions, the relation between mineral and rock composition versus BCC or DSC color is predictable and has been largely used in this study to identify and map geologic materials. The SPOT panchromatic image (Figure 5) and the BCC and DSC images were used with a stereoscope to determine the morphological characteristics of each exposure. These data were also used to determine fine-scale spatial relations of exposures. The natural-color image (Figure 4) was used mostly to determine material differences based on brightness of the exposures.

The list of geologic units on Sheet 1 is in order of increasing age from top to bottom, as inferred from superposition relations determined from the SPOT and BCC or DSC stereo-image pairs. This section briefly describes the remote-sensing characteristics that were used to discriminate the geologic map units.

Stippled pattern - Playa and high-albedo alluvial deposits. The unit has very high albedo (white in natural color) and flat to negative topography. Most and possibly all of these deposits are playas. Many of these deposits have either clay or adsorbed water at the surface as indicated by their blue color on the BCC and DSC images.

Qa - Quaternary alluvium, colluvium, and eolian deposits. We did not discriminate between these three types of unconsolidated deposits because (1) their physical properties are very similar, (2) their distinction on the geologic map would have greatly complicated the map's interpretability, and (3) their distinction in certain locations would have been difficult or impossible. These deposits have a wide range of colors on the BCC and DSC images because their color is controlled by material provenance that ranges from local to area-wide.

gb - Gabbro. Gabbro is exposed only in the northeast corner of the map area. This unit is of Triassic age according to a published geologic map (Borovikov, 1972). The gabbro exposures have a brown color on the BCC image and appear as low-lying mounds, weathered to rounded shapes.

t - Tuffaceous deposits. This unit is widespread within the study area. Borovikov's (1972) map suggests that there are several tuffaceous units of different Paleozoic ages. We could not determine if the tuffs are younger or older than the granite and granodiorite intrusions. We believe, however, that the tuff deposits are younger than the Paleozoic metasedimentary units that occur within the study area. We could distinguish three tuffaceous units around Degelan Mountain (Figure 4) based on their color, which ranges from blue (mostly cyan) to green to yellow from the top to the bottom of an exposure. We did not distinguish these different tuff units on the geologic map (Sheet 1), which is at too small a scale to show this level of detail. Generally, the tuffs are flat lying and form mesas or buttes except where the beds have been tilted by folding and faulting (north of Degelan Mountain). The relief of the tuff is subdued because tuff easily erodes to form dissected (badlands) terrain.

tc - Tuffaceous deposits thinly covering bedrock. Some exposures of tuff appear to be so thin that they assume the morphology of the underlying bedrock.

g- Granite. Scattered throughout the study area are granite plutons that characteristically have a yellowish-pink color on the BCC or DSC images, high relief, sharp ridges resulting from dense jointing and faulting, sharp contacts, and possibly contact-metamorphism aureoles. One of these plutons is Degelan Mountain (Figure 4).

gd - Granodiorite. The large exposures of granodiorite in the study area

characteristically have a yellowish-pink color on the BCC or DSC images (similar to granite), very low relief, hummocky texture resulting from dense jointing and faulting, and gradational contacts. Most exposures appear to be partly coated or covered by maroon- or blue-colored metasedimentary or sedimentary rock.

q - Quartzite. A few exposures of quartzite occur in the southwest and southeast corners of the study area. They have a yellow-brown color on the BCC and DSC images, fairly high relief, and sharp ridges (apparently resistant to erosion); they lack distinct bedding.

The remainder of the rock exposures in the study area consist of metasedimentary rocks of Paleozoic age. These units are distinguished on the basis of color on both the BCC and DSC images. All four units have moderate relief and faint to distinct bedding; most are folded and faulted.

Ps - Paleozoic metasedimentary rocks, siliceous. This unit has a large percentage of quartz and originally may have been a siltstone or sandstone. Its red color on the BCC and DSC images suggests that it has appreciable amounts of ferric oxide.

Pc - Paleozoic metasedimentary rocks, carbonate/sulfate. The high percentages of carbonate or sulfate minerals display absorptions within or near the wavelength regions of TM bands 4 and 7, which produces the blue color on the BCC and DSC images.

Pcl - Paleozoic metasedimentary rocks, clay-rich. The high percentage of clay minerals, whose spectral reflectance is characteristically low in TM bands 1 and 7, results in a green color on the BCC and DSC images.

Pf - Paleozoic folded and faulted metasedimentary rocks, undivided. This unit has all the morphologic characteristics of the other metasedimentary units, but its exposures are too small to accurately determine its color on the BCC and DSC images.

ANALYSIS OF STRUCTURAL GEOLOGY

We mapped the structural geology in the Semipalatinsk region (Sheet 2) using all the image data shown in Figures 3-9. The stereopair combination of TM and SPOT was extremely valuable in this respect, because these data amplify relief and allow better determination of direction of vertical displacements. The BCC image of the entire TM scene (Figure 3) was very useful in establishing regional fault trends. We could not determine from the remotely sensed image data the amount of dip along the faults, nor could we discriminate between normal and reverse faulting. However, given the tectonic history of this region, as summarized in the introduction, thrust faults should be present.

We used several morphologic and geologic factors to determine the existence and

direction of faulting and folding shown on Sheet 2. These factors include the following:

1. Deflected or straight stream channels
2. Straight contacts between erosional and depositional features
3. Straight valleys in bedrock areas
4. Linear alignments of vegetation
5. Linear features crossing drainage channels
6. Topographic scarps
7. Distinct hue or tonal changes on opposite sides of a lineament
8. Lineaments traceable from bedrock to adjoining surficial materials
9. Offsets in drainage channels, topographic features, and geologic contacts

ANALYSIS OF DRAINAGE

The type of drainage system that develops on local and regional surfaces is largely controlled by slope, type of soil or surficial deposit (texture and thickness), and the type and attitude of surface and buried rock bodies. Consequently, drainage was studied and classified according to its (1) pattern and (2) texture or density to assist in the geologic (lithology and structure) analysis of the Semipalatinsk region. All computer-enhanced TM and SPOT images previously described (Figures 3-9) were interpreted to compile a 1:150,000-scale drainage map showing both patterns and textures (Sheet 3).

On the TM and SPOT images, sixteen diagnostic drainage patterns were recognizable because of their geometric attributes (Parvis, 1950; Way, 1973; Avery and Berlin, 1991). These patterns are shown on Sheet 3 and defined below.

(A) Radial-Centripetal: Develops where streams flow radially inward and downward toward a basin or depression such as a playa. This form is common in dry regions and indicates basin formation or subsidence.

(B) Radial-Centrifugal: Develops where streams flow radially outward and downward in all directions from the central part of a symmetrical hill or mountain (e.g., structural dome, granitic pluton) unless altered by structural control.

(C) Annular: Develops where subsequent streams adjust their courses to follow a curved path around the base of resistant hills. Their courses commonly intercept radial streams associated with well-dissected domes and domal anticlines; their exact basal form is controlled by the topography.

(D) Dendritic: Characterized by a random, tree-like branching system in which the tributaries joint the gently curving main stream at acute angles. It is indicative of relatively homogeneous soil or rock materials (i.e., same resistance to erosion) with little or no structural control. The pattern is typified by high-relief landforms composed of massive crystalline rocks.

(E) Modified Trellis: Characterized by two orthogonal sets of straight and parallel stream courses; the dominant set follows a series of strike valleys. whereas the second set follows cross faults or eroded fracture zones. This pattern is a right-angle system and is structurally controlled.

(F) Dichotomic: Develops on alluvial slopes such as alluvial fans and bajadas. The stream courses fan out, distributing the flow from the main, headward channel through a series of branching distributary channels, which may show braided characteristics. Runoff normally disappears into coarse, granular sediments (high permeability).

(G) Angulate: A variation of the dendritic or trellis systems. Tributaries tend to parallel one another, and the angle at which they join the next higher order stream course is acute or obtuse. This form develops when the stream courses follow fracture, fault, or joint patterns in the underlying bedrock.

(H) Parallel: Characterized by a series of stream courses that are parallel or nearly parallel; they characteristically join a main stream at about the same angle. This pattern can develop where streams are formed on uniformly sloping surfaces of the same fine-textured surficial material or along parallel faults or fracture zones in hard, resistant bedrock.

(I) Asymmetrical: A form in which more tributaries enter a main stream from one side than from the other, the upslope and downslope sides, respectively. This pattern is often found in folded strata and mountainous terrain.

(J) Braided: Develops on broad, graded streams and is controlled by the stream's own deposited load; the pattern consists of an intricate network of shallow, shifting channels. This pattern usually indicates that the materials deposited in the stream channels are coarse and permeable.

(K) Contorted: Associated with a stream that changes direction abruptly, having deviated or been deflected from its normal course; this pattern indicates control by a fault, fold, or lithologic barrier.

(L) Internal: Indicates the lack of an integrated drainage system. It can be associated with a relatively young landform with minimal relief, with granular materials having high permeability, or with porous rocks.

(M) Anomalous: Suggests the existence of important geological conditions. The following anomalous patterns were identified in the study area:

M1: Long, straight stream-course segments suggestive of a buried fault or fracture zone.

M2: Special alignment of stream courses (e.g., drainage offsets), which suggest control by a strike-slip fault.

M3: Downstream narrowing of alluvial valleys suggesting the presence of more resistant rock or a local structure.

M4: Anomalous alluvial buildups, sometimes called alluvial ponding, often occur immediately upstream from a lithologic or structural barrier; such buildups are commonly associated with compressed meanders, further indicating a reduction in stream gradient.

The drainage patterns were further classified by variations in texture or channel density per unit area. Three categories were identified, and representative examples are shown on Sheet 3.

(1) Fine-textured drainage has a high drainage density (closely spaced channels) and typically indicates high levels of surface runoff, relatively impervious and easily eroded bedrock, and surficial materials of low permeability.

(2) Medium-textured drainage has a moderate drainage density (moderately spaced channels) and develops on surficial deposits and bedrock having a moderate permeability.

(3) Coarse-textured drainage has a low drainage density (widely spaced channels) and develops on pervious rock formations and highly permeable surficial materials, such as sand and gravel, because little water is available as surface runoff.

SUMMARY ANALYSIS

Our mapping of the Semipalatinsk region is consistent with the pertinent Soviet geologic literature. In particular, our geologic map generally corroborates the published geologic map of Barovikov (1972), although our maps are more detailed by at least an order of magnitude. The following combination of our mapping of the geology (Sheet 1), structure (Sheet 2), and drainage (Sheet 3) are based on a set of general observations and conclusions.

1. The integrated geologic setting of this region is very similar to that of the Nevada Test Site. The Semipalatinsk study area has a semi-arid to arid climate and contains mostly playa and tuff deposits and folded and faulted Paleozoic metasedimentary rocks. The Shagan River, which bisects the area, seems to be fault controlled. There is also a north-trending fault that divides Yucca Valley within the Nevada Test Site. If the "Shagan River fault" is dip-slip, the west side is the downthrown block; the thickness of sediments within the river valley could be between 100 m and 1000 m if it is similar to sediment thicknesses reported for surrounding areas (Zonenshain et al., 1990).

2. The geology of the Semipalatinsk area differs from that of the Nevada Test Site in two respects. First, siliceous plutonism occurred at Semipalatinsk, whereas mafic volcanism occurred at the Nevada Test Site. In addition, the tuffs of the Semipalatinsk area are of Paleozoic age, whereas the tuffs within the Nevada Test Site are all Tertiary in age. Second, the tectonism in the Semipalatinsk area is a mixture of dip-slip and strike-slip faulting (i.e., Appalachian-style tectonism), whereas in the Nevada Test Site the tectonism is dip-slip (i.e., Basin-and-Range-style tectonism).

3. The two major fault systems in the Semipalatinsk area trend northwest and northeast. The latter appears to be older because its tectonic indicators are more degraded. This observation is consistent with published literature, in which the earlier tectonism (Caledonian) is considered to have produced mostly northeast-trending faults and the later tectonism (Hercynian) is thought to have produced mostly northwest-trending faults. The large strike-slip fault in the southwest corner of the study area (Figure 3 and Sheet 2) is probably a segment of the major Chingiz fault system.

4. Our mapping suggests that the layered units that are colored red and blue on the BCC and DSC images represent red sandstone and limestone beds, respectively, which have been metamorphosed during various tectonic events. The blue metasedimentary aureoles around most of the granite intrusions indicate that the limestone is beneath and older than the sandstone. Published literature (Nalivkin, 1960, 1973; Rotarash et al., 1980, 1982; Zonenshain et al., 1990) corroborates our remote-sensing results in regard to both rock type and

stratigraphic relations: according to these workers, the early sedimentary rocks were mostly carbonates and the later sedimentary rocks were mostly red sandstones and shales. During the Salairide Orogeny (Late Cambrian), granitic intrusions metamorphosed and folded limestone country rock in nearby locations (Zonenshain et al., 1990). Although the granitic intrusions within the Semipalatinsk area are of late Carboniferous and Permian age, the same contact metamorphic effects are seen around most of these intrusions.

5. The large fold belt in the Semipalatinsk area consists mostly of Paleozoic metasedimentary rocks. The northwest-trending axis of the fold belt is parallel to the trend of the major fault system that formed during the Hercynian tectonic period, in which the Kazakstan and Siberian plates collided.

6. Generally, the type of drainage within exposures of each major rock unit is consistent for that unit. Radial-centrifugal drainage occurs mostly on the granitic intrusions because they are generally domical. Internal drainage occurs on the granodiorite intrusions, which implies that the low-lying exposures have been intensely fractured. Dichotomic drainage occurs mostly on the tuffaceous deposits, which corroborates their permeable nature. Modified trellis drainage is found mostly on the metasedimentary rock units, which is the result of the orthogonal directions of the bedding and faulting.

ACKNOWLEDGEMENTS

This work was supported by the Department of Energy, Office of Arms Control, under contract W-7405-ENG-36. The authors thank Thomas Weaver for his valuable comments and suggestions.

REFERENCES CITED

Avery, T. E., and G. L. Berlin, 1991, Fundamentals of Remote Sensing and Airphoto Interpretation, 5th Edition, Macmillan Publishing Co., New York, in press.

Borovikov, L. E. (Editor), 1972, Tectonic Map of Central and Eastern Kazakstan, scale 1:1,100,00, Sheet 2.

Chavez, P. S., 1988, An improved dark-object subtraction technique for atmospheric scattering correction of multispectral data, Remote Sensing of Environment, v. 24, p. 459-479.

Chavez, P. S., G. L. Berlin, and L. B. Sowers, 1982, Statistical method for selecting Landsat MSS ratios, J. Applied Photographic Engineering, v. 8, p. 23-30.

Crippen, R. E., 1989, Selection of Landsat TM band and band-ratio combinations to maximize lithologic information in color composite displays, Proceedings Seventh Conference on Remote Sensing for Exploration Geology, Environmental Research Institute of Michigan, p. 917-921.

Davis, P. A., and G. L. Berlin, 1989, Rock discrimination in the complex geologic environment of Jabal Salma, Saudi Arabia, using Landsat Thematic Mapper data, Photogrammetric Engineering and Remote Sensing, v. 55, p. 1147-1160.

Davis, P. A., G. L. Berlin, and P. S. Chavez, 1987, Discrimination of altered basaltic rocks in the southwestern United States by analysis of Landsat Thematic Mapper data, Photogrammetric Engineering and Remote Sensing, v. 53, p. 45-55.

Esenov, S. E. (Editor), 1971, Geologic Map of Central Kazakstan, scale 1:1,500,000.

Gillespie, A. R., A. B. Kahle, and R. E. Walker, 1986, Color enhancement of highly correlated images. I. Decorrelation and HSI contrast stretches, Remote Sensing of Environment, v. 20, p. 209-235.

Khain, V. E., 1985, Geology of the U.S.S.R.: First Part -- Old Cratons and Paleozoic Fold Belts, Gebruder Borntraeger, Berlin, 272 p.

Nalivkin, D. V., 1960, The Geology of the U.S.S.R., A Short Outline (incl. a 1:7,500,000-scale geologic map), Pergamon Press, New York, 170 p.

Nalivkin, D. V., 1973, Geology of the U.S.S.R., University of Toronto Press, Toronto, 855 p.

Parvis, M., 1950, Drainage pattern significance in airphoto identification of soils and bedrocks, Photogrammetric Engineering, v. 16, p. 387-409.

Rotarash, I. A., and Ye. A. Gredyushko, 1980, Development and structure of serpentinite melange in the Zaisan folded region (translated), Geotectonics, v. 14, p. 234-237.

Rotarash, I. A., N. A. Klepikov, and Ye. A. Gredyushko, 1980, Lower Paleozoic olistostromes of the Chingiz-Tarbagatay anticlinorium (translated), Geotectonics, v. 14, p. 283-288.

Rotarash, I. A., S. G. Samygin, Ye. A. Gredyushko, G. A. Keyl'man, V. S. Mileyev, and A. S. Perfil'yev, 1982, The Devonian active continental margin in the southwestern Altay (translated), Geotectonics, v. 16, p. 31-41.

Rotarash, I. A., and L. M. Trubnikov, 1983, Rudnyi Altai volcanic belt (translated), Geology and Geophysics, v. 24, p. 24-29.

Rumney, G. R., 1968, Climatology and the World's Climate, Macmillan Company, New York, 656 p.

Sheffield, C., 1985, Selecting band combinations from multispectral data, Photogrammetric Engineering and Remote Sensing, v. 51, p. 681-687.

UNESCO, 1977, Map of the World's Distribution of Arid Regions and Explanatory Note, scale 1:25,000,000, United Nations, Paris, 54 p.

Way, D.S., 1973, Terrain Analysis, Dowden, Hutchinson, and Ross, Stroudsburg, Pennsylvania, 392 p.

Zonenshain, L. P., M. I. Kuzmin, and L. M. Natapov, 1990, Geology of the U.S.S.R.: A plate-tectonic synthesis, (B. M. Page, Ed.), American Geophysical Union Geodynamics Series, v. 21, 242 p.

Figure 1. Index map of Asia showing the location of the Semipalatinsk study area.

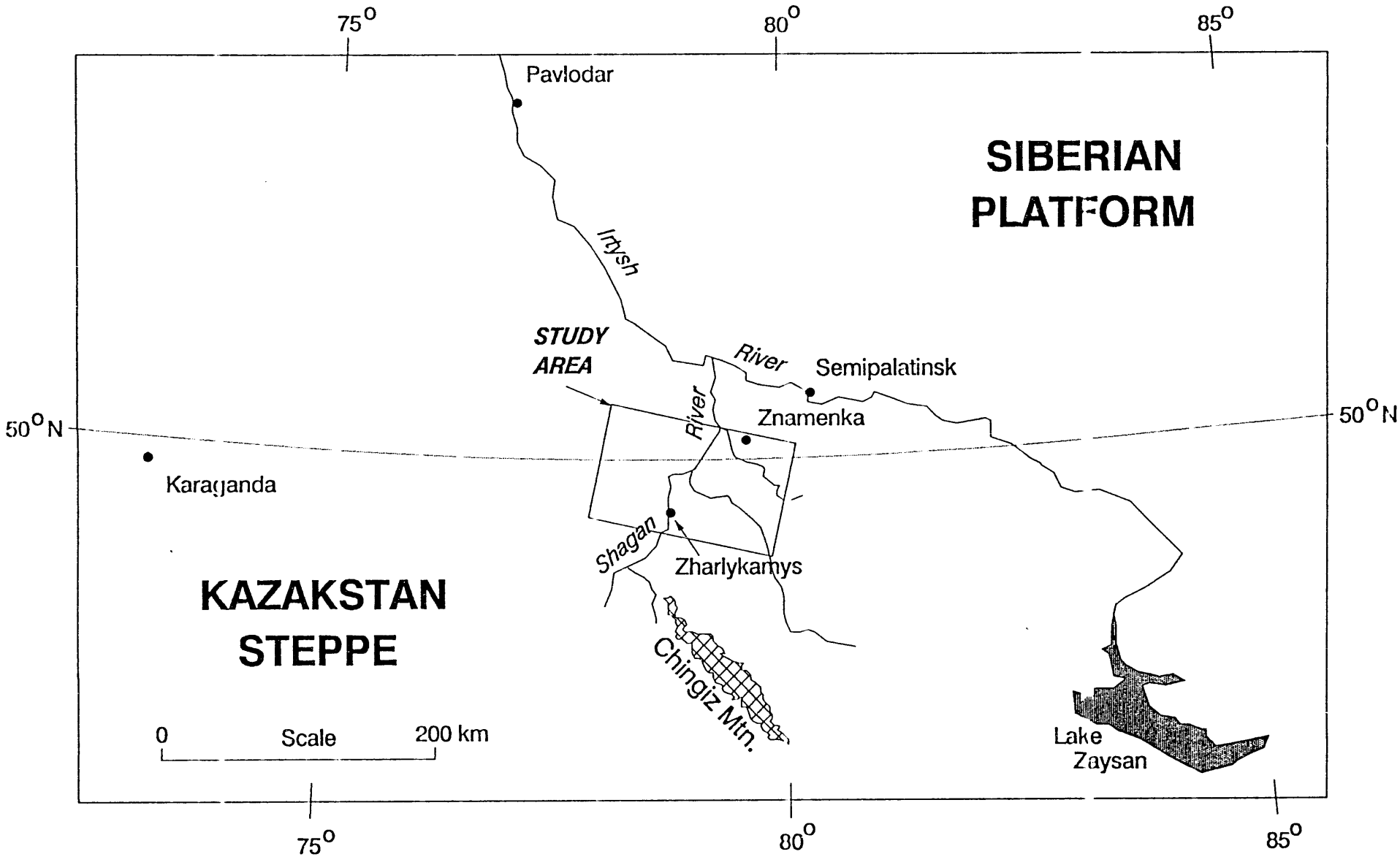

Figure 2. Index map of eastern Kazakstan showing location of the study area.

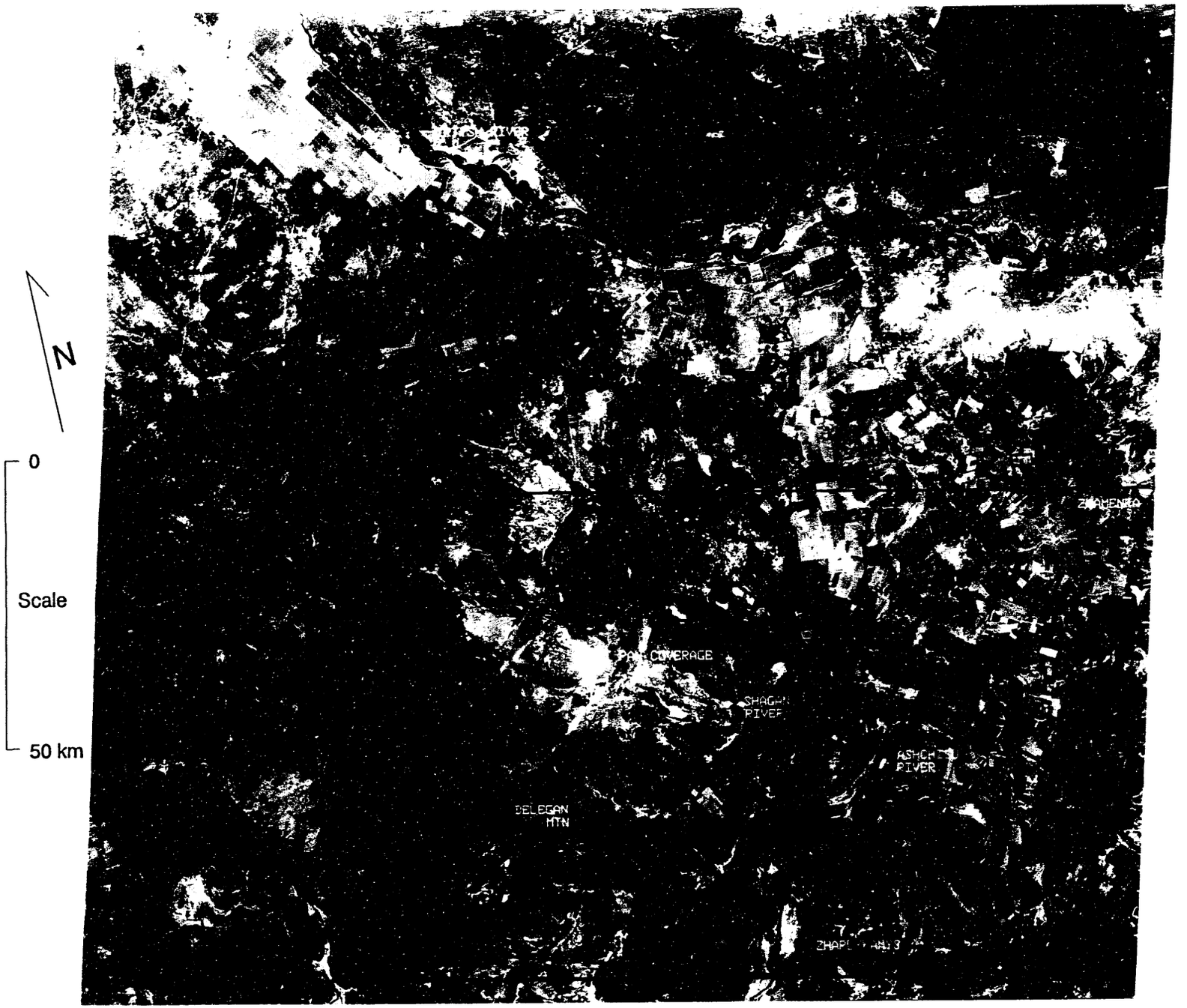

Figure 3. TM-band color-composite (BCC) image of TM scene 42575-05110. TM band 1 displayed as blue, 4 as green, and 7 as red. Large rectangle is the study area; smaller rectangle is the coverage of the SPOT image used in our analysis.

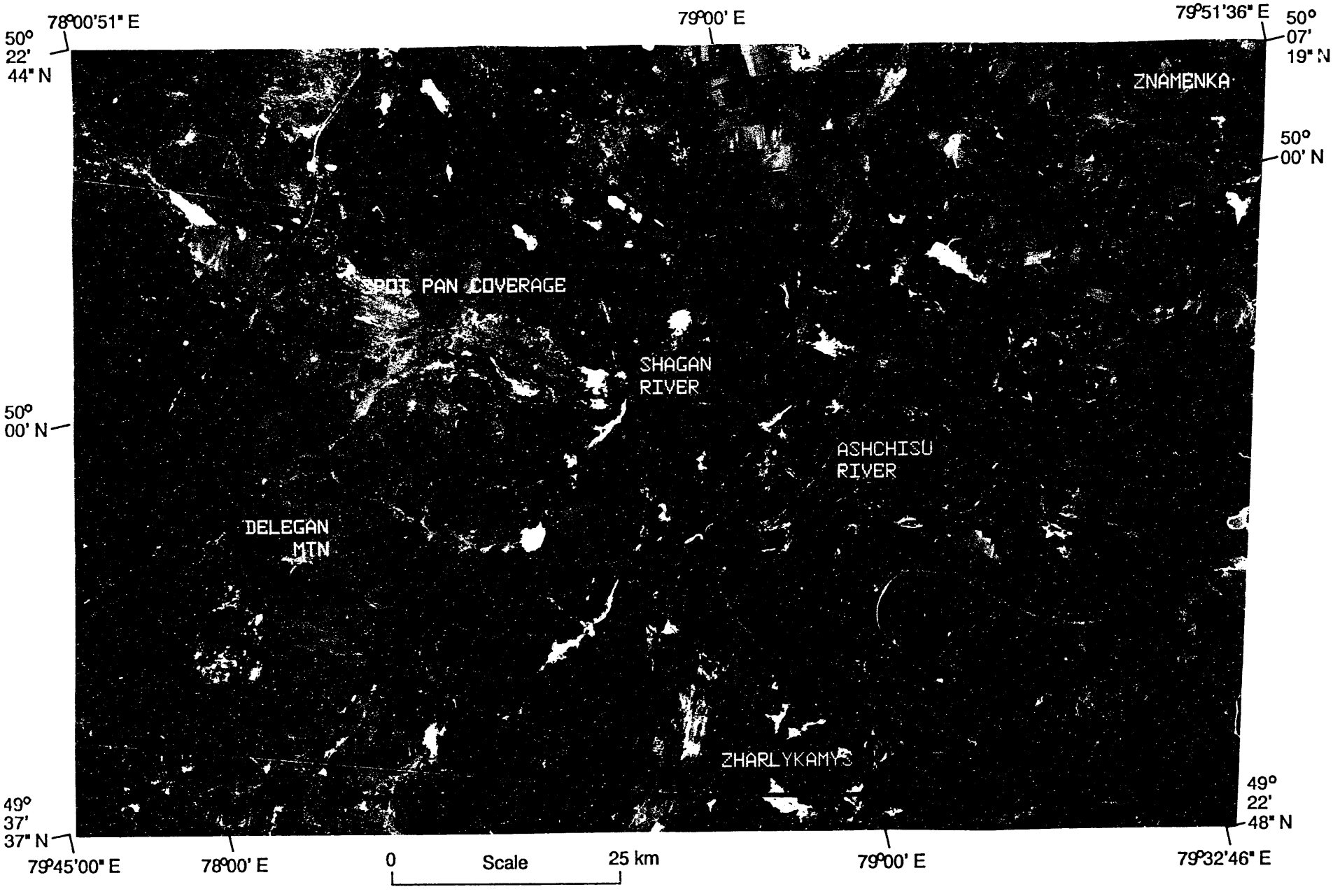

Figure 4. TM natural-color composite image of the Semipalatinsk study area: TM band 1 displayed as blue, 2 as green, and 3 as red. Area defined by yellow lines indicates the areal coverage of SPOT 10-m panachromatic data that was used to refine our interpretations.

MAP SHOWING THE SURFACE GEOLOGY
OF THE SEMIPALATINSK REGION,
EASTERN KAZAKSTAN (SHEET 1 OF 3)

78° 00′51″E

50° 22′44″N

gd
Qa
gd
Pc
Ps
Pc
Qa
Pc
Ps
Ps
Pc

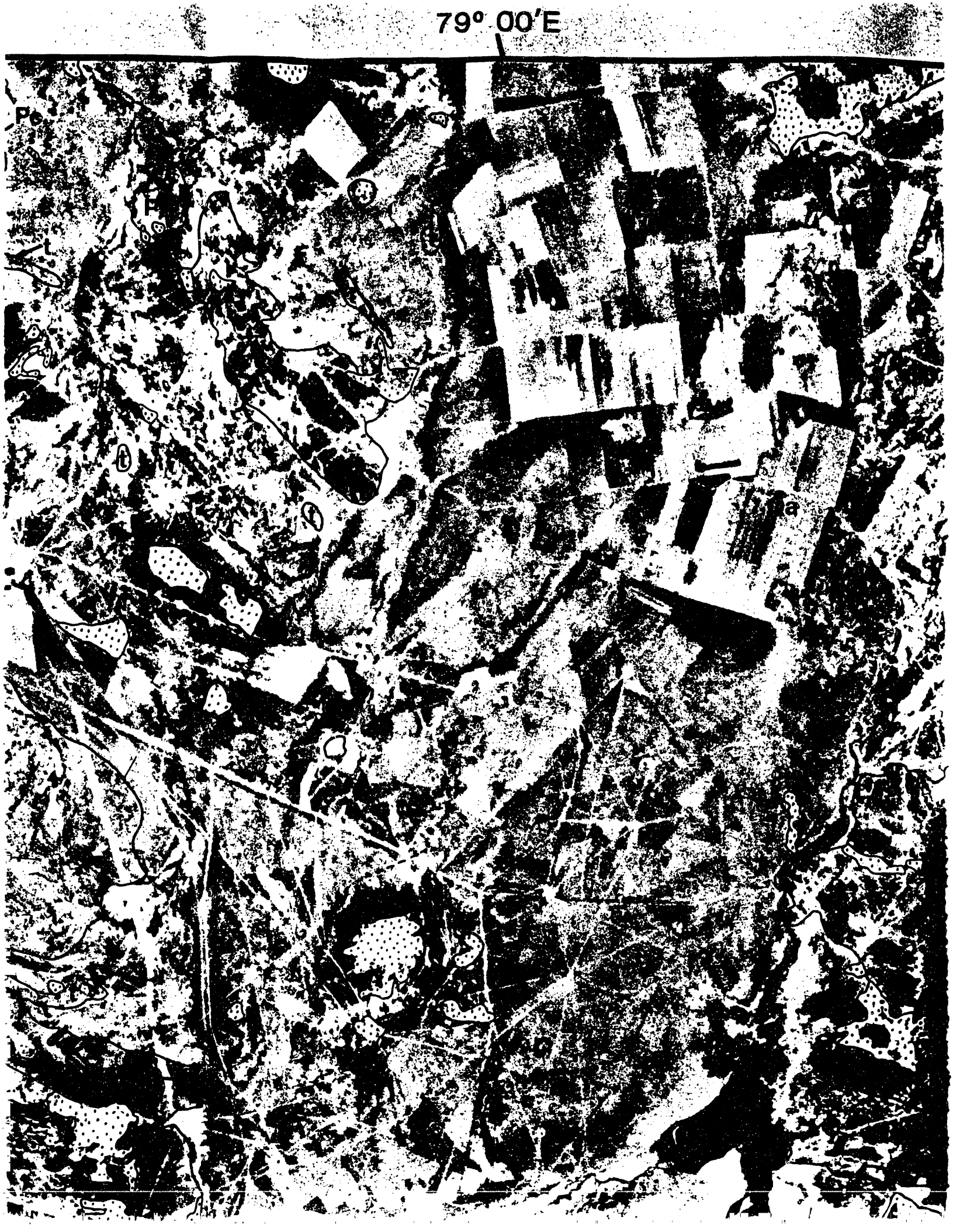
79° 00'E

Pc
t
Ps
Ps
Pc
Qa
Ps
Ps
Ps
Ps
Ps
Ps
Ps

79° 51′36″E
50° 07′19″N
50° 00′N
Pc
gb
t
Ps
Pc
Pc
Pc
g
t

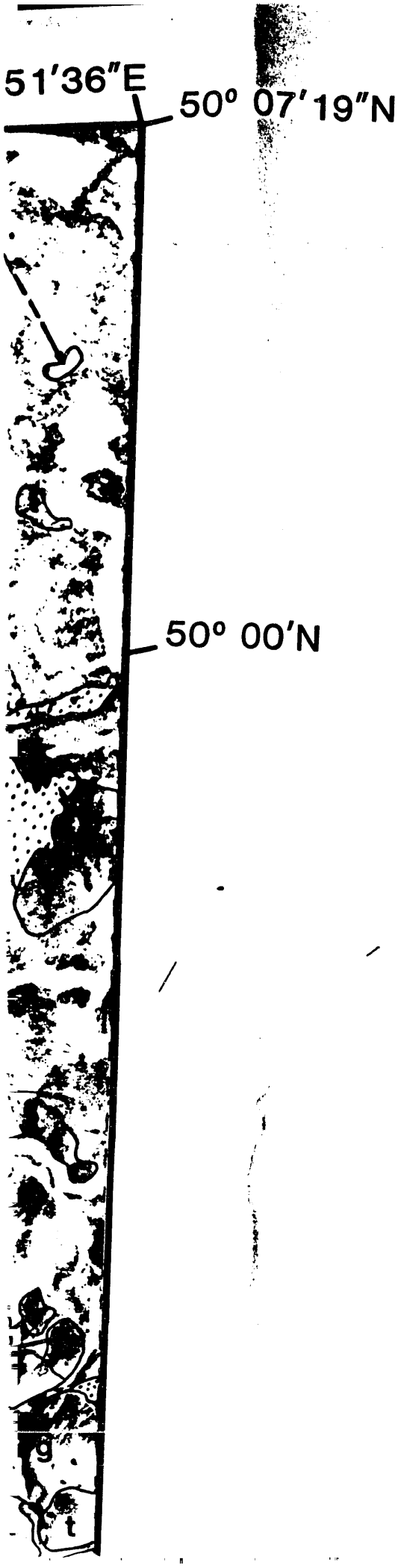

MAP SHOWING THE SURFACE GEOLOGY OF THE SEMIPALATINSK REGION, EASTERN KAZAKSTAN (SHEET 1 OF 3)

50° 00'N

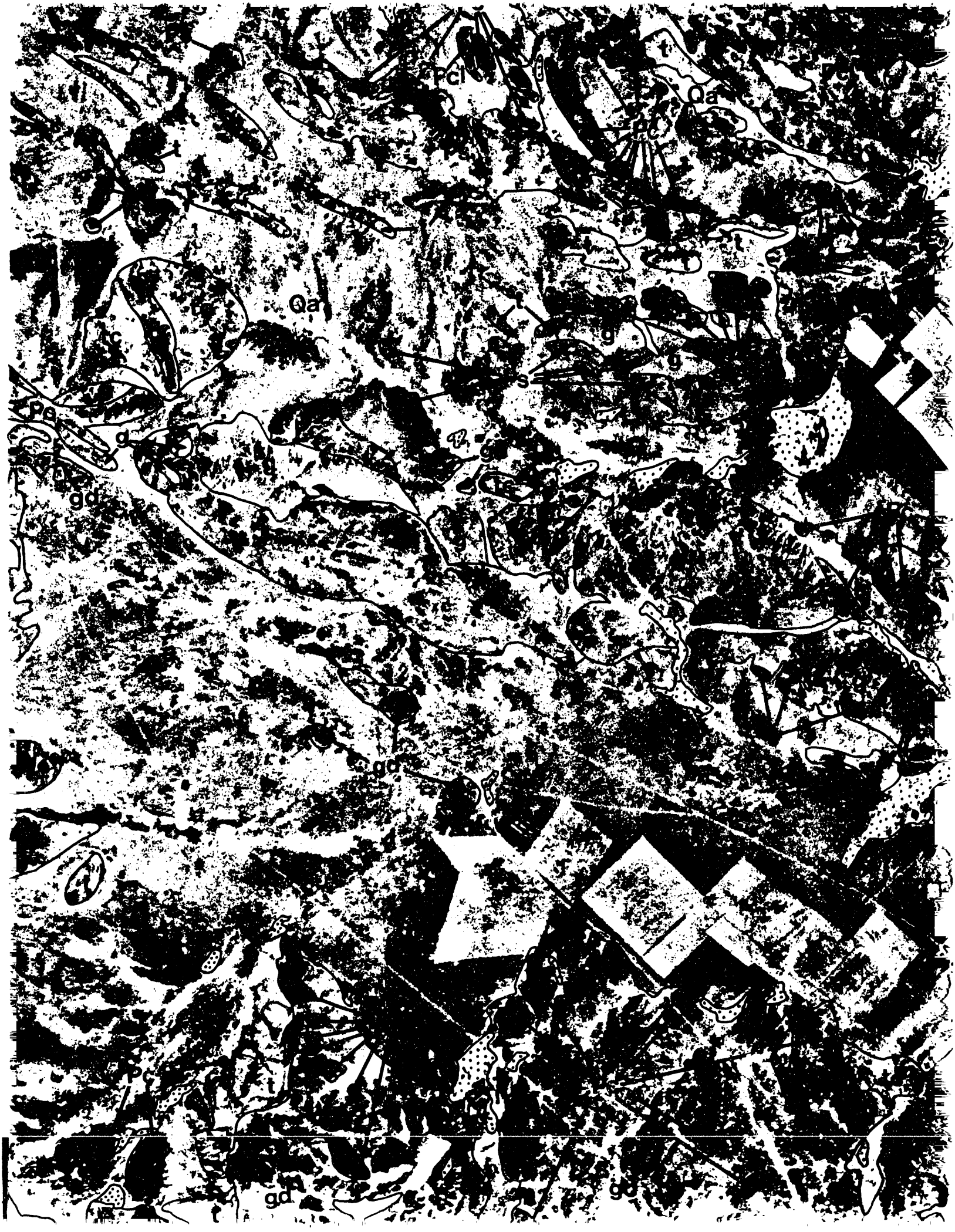
Pcl
Qa
Qa
Pe
gd
gd
gd
gd

PG

LIST OF M

	Quaternary playa anc
Qa	Qaternary alluvium, c
gb	Gabbro weathered ar
t	Tuffaceous deposit. varied relief; easily er
tc	Tuffaceous deposit th
g	Granite. High relief, s
gd	Granodiorite. Low re
q	Quartzite
Ps	Paleozoic metasedim
Pc	Paleozoic metasedim
Pcl	Paleozoic metasedim than other metasedin
Pf	Paleozoic folded and
	Standing water

LIST OF MAP UNITS

	Quaternary playa and high-albedo alluvial deposits
Qa	Qaternary alluvium, colluvium, and eolian deposits
gb	Gabbro weathered and eroded to smooth, low-relief mounds
t	Tuffaceous deposit. Composition ranges from siliceous to mafic; varied relief; easily eroded; forms mesas, rounded hills, and incised scarps
tc	Tuffaceous deposit thinly covering bedrock, assumes morphology of bedrock
g	Granite. High relief, sharp outlines, highly faulted
gd	Granodiorite. Low relief, dissected morphology
q	Quartzite
Ps	Páleozoic metasedimentary rocks, siliceous. Folded and faulted
Pc	Paleozoic metasedimentary rocks, carbonate/sulfate. Folded and faulted
Pcl	Paleozoic metasedimentary rocks, clay-rich. Folded and faulted; more eroded than other metasedimentary rocks
Pf	Paleozoic folded and faulted metasedimentary rocks, undivided
	Standing water

Base is Landsat Thematic Mapper band 4.

Geology was mapped using Landsat Thematic Mapper true-color and false-color image products.

5

MAP SHOWING THE SURFACE GEOL

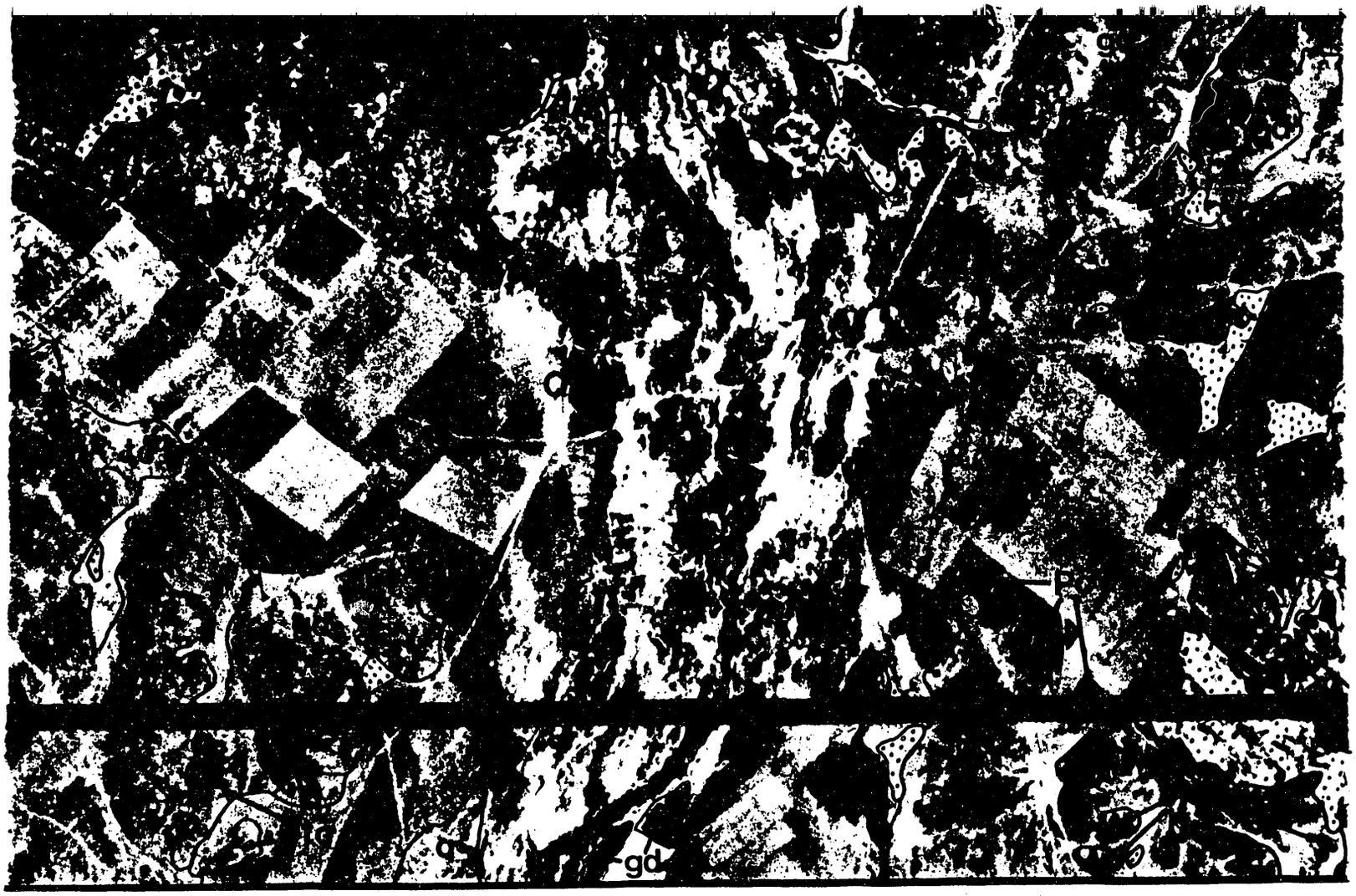

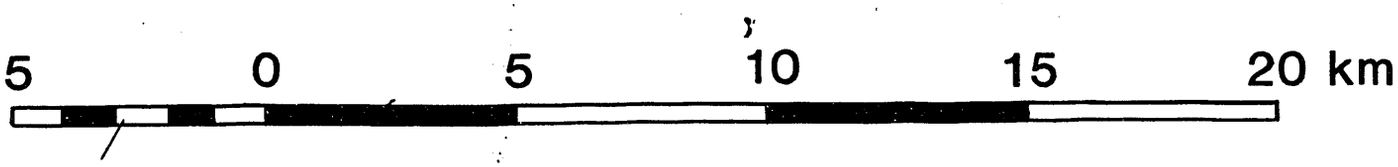

Scale 1:150,000

GEOLOGY IN THE SEMIPALATINSK REGIO

By

Philip A. Davis and Graydon L. Berlin

79° 00′E

ION, EASTERN KAZAKSTAN

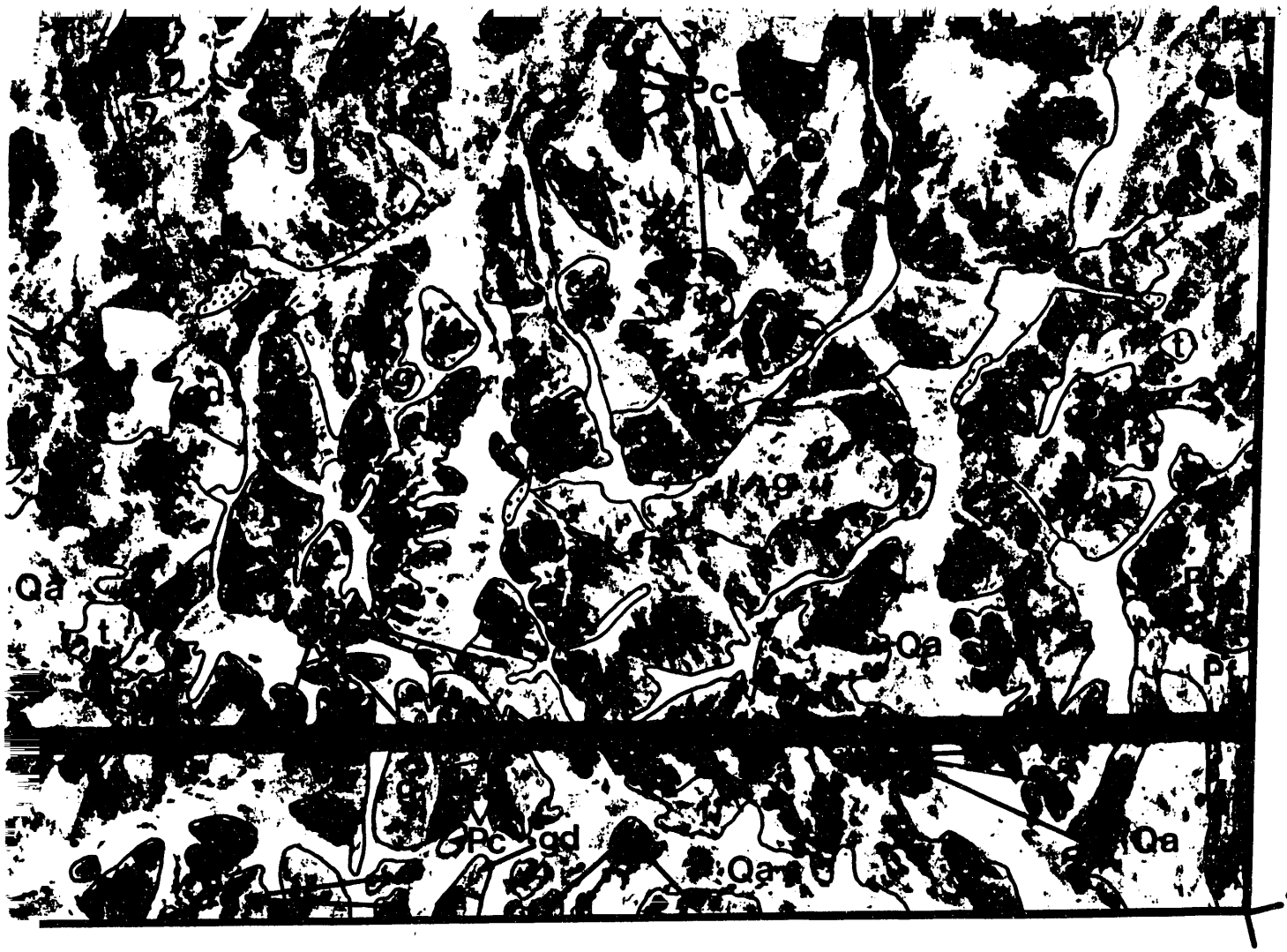

49° 22′

79° 32′46″E

Standing water

49° 22′48″N

2′46″E

MAP SHOWING THE STRUCTURAL GEOLOGY IN THE SEMIPALATINSK REGION, EASTERN KAZAKSTAN (SHEET 2 OF 3)

49° 22′48″N

′46″E

49° 22′48″N

79° 32′46″E

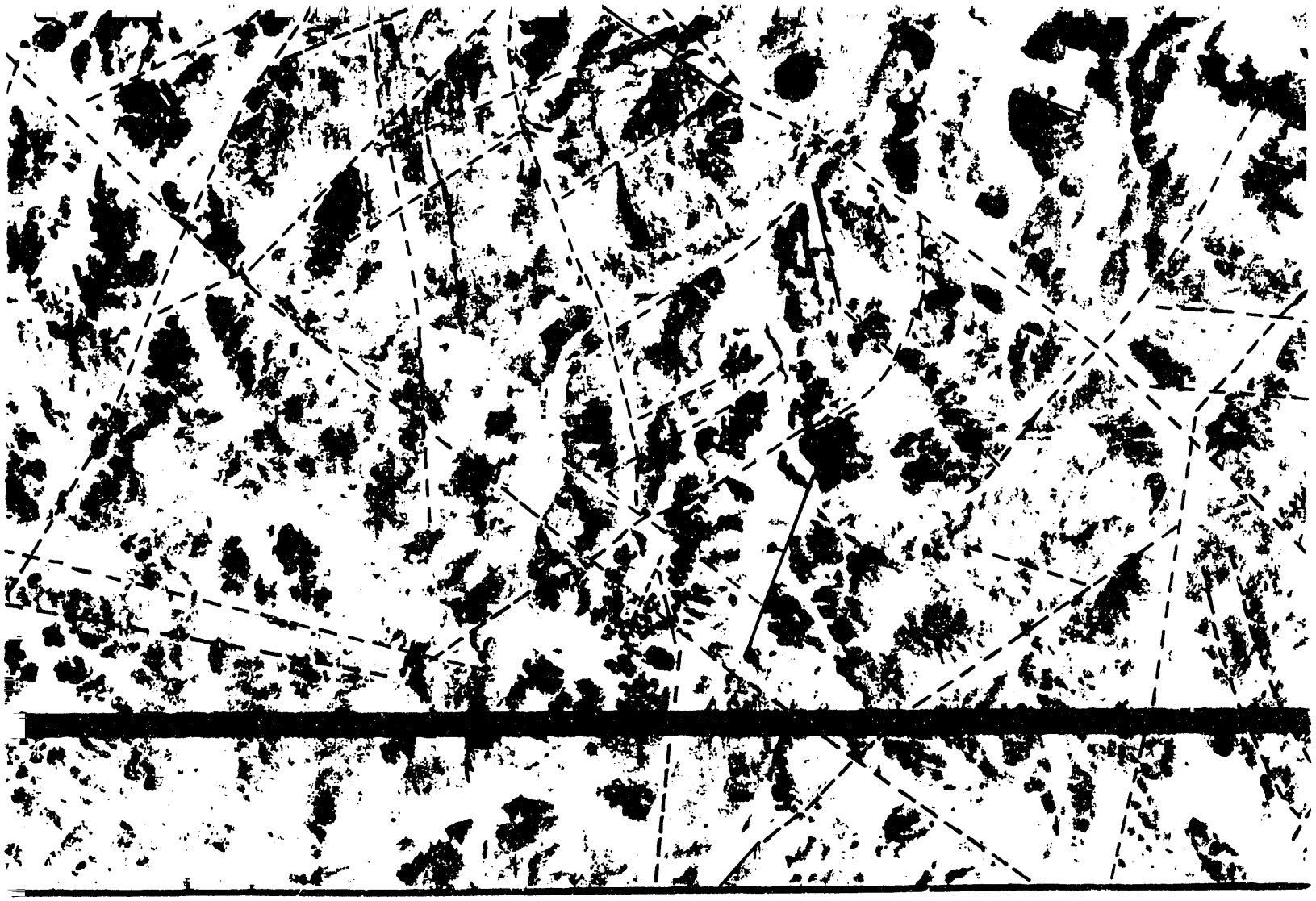

ZAKSTAN

78° 00′51″E

50° 22′44″N

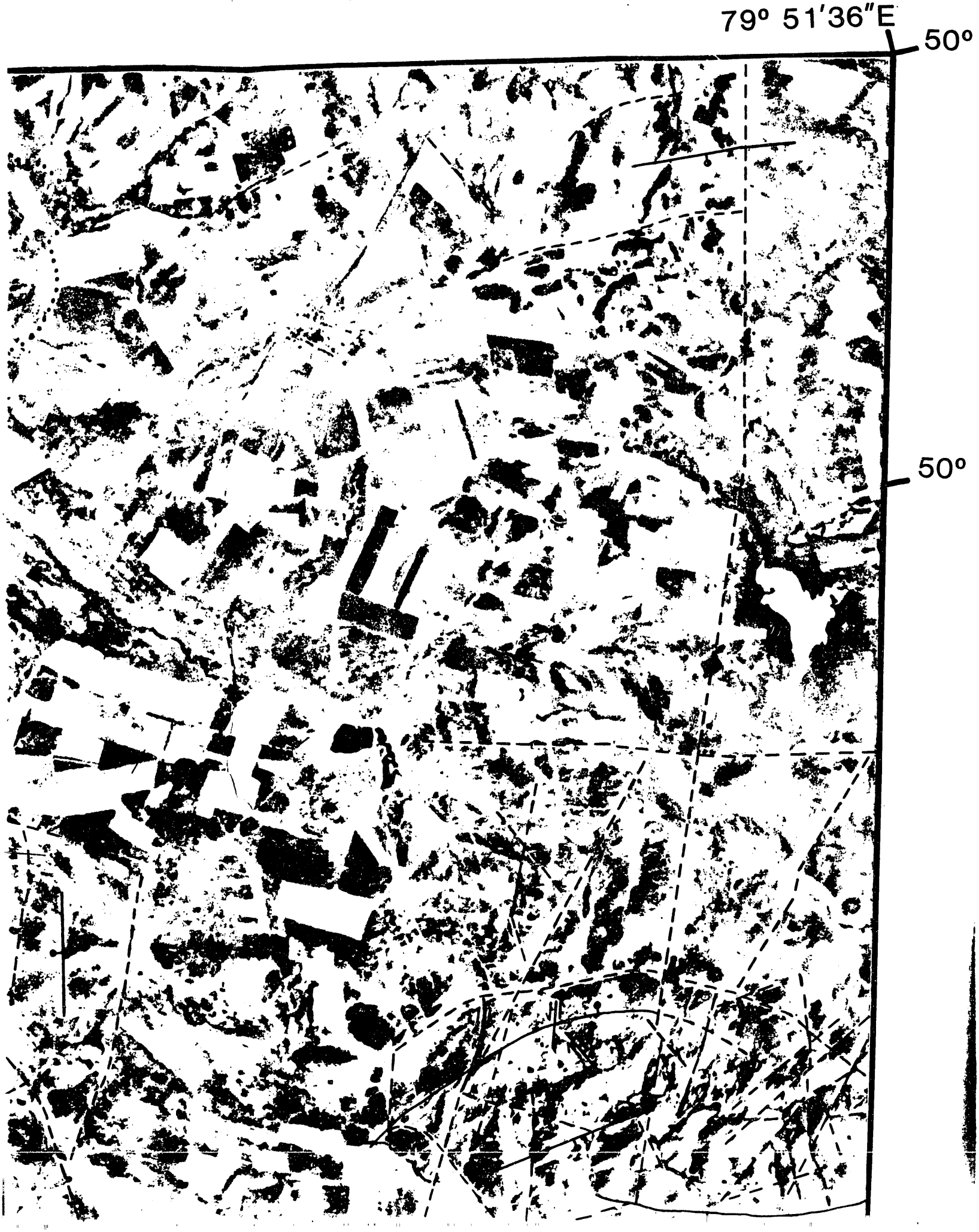
79º 51′36″E
50º
50º

MAP SHOWING THE STRUCTURAL GEOLOGY IN THE SEMIPALATINSK REGION, EASTERN KAZAKSTAN (SHEET 2 OF 3)

EXPLANATION OF LINE SYMBOLS

49° 37′37″N

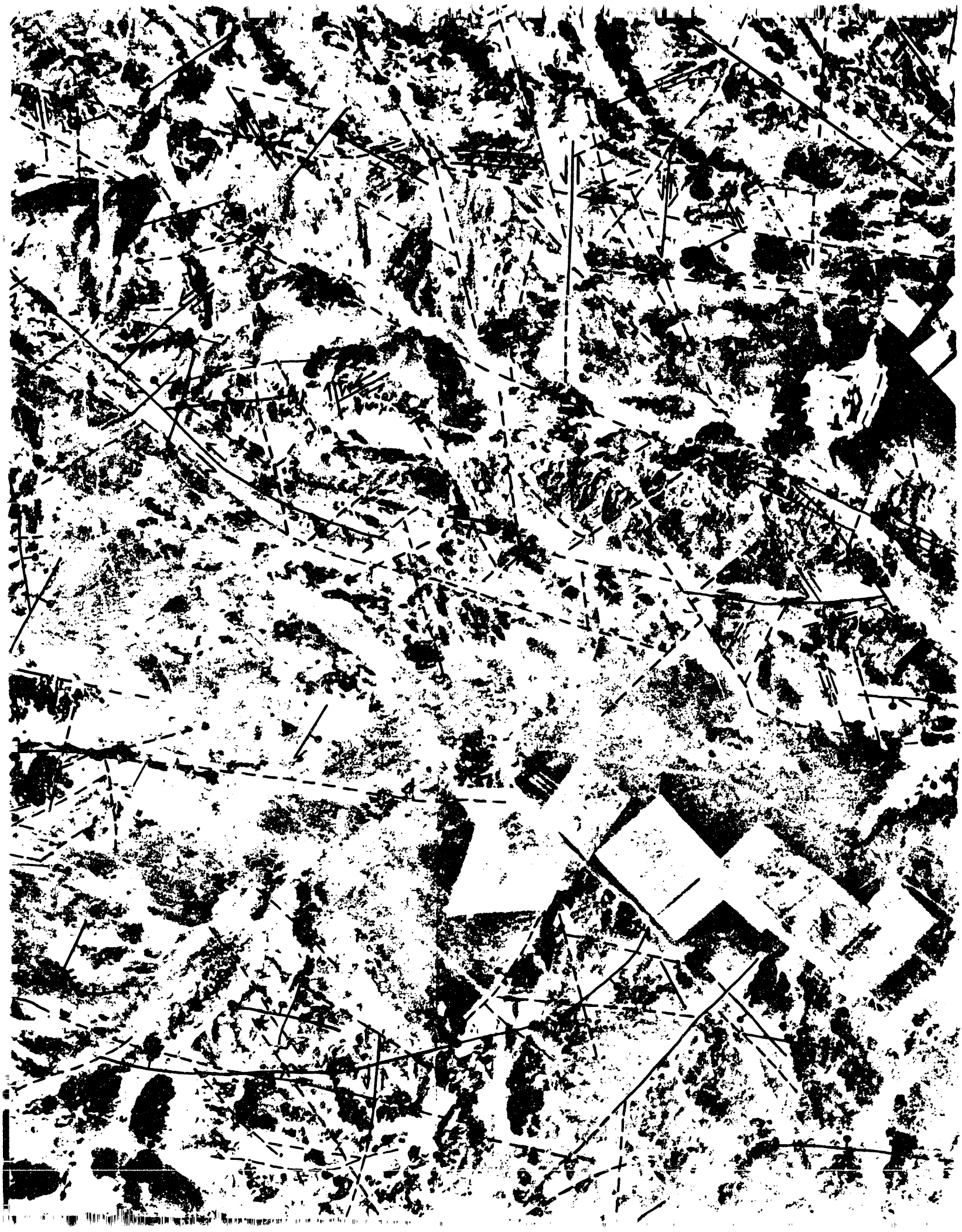

EXPLANA

Escarpmen

Geomorph

Strike and

Beds near

Fault, pro
side

Fault, sho

Dome

Escarpment, hachures point downslope

Geomorphic positive anomaly

Strike and dip, amount of dip cannot be determined

Beds near vertical dip

Fault, probable or possible; ball on downthrown side

Fault, showing relative horizontal movement

Dome

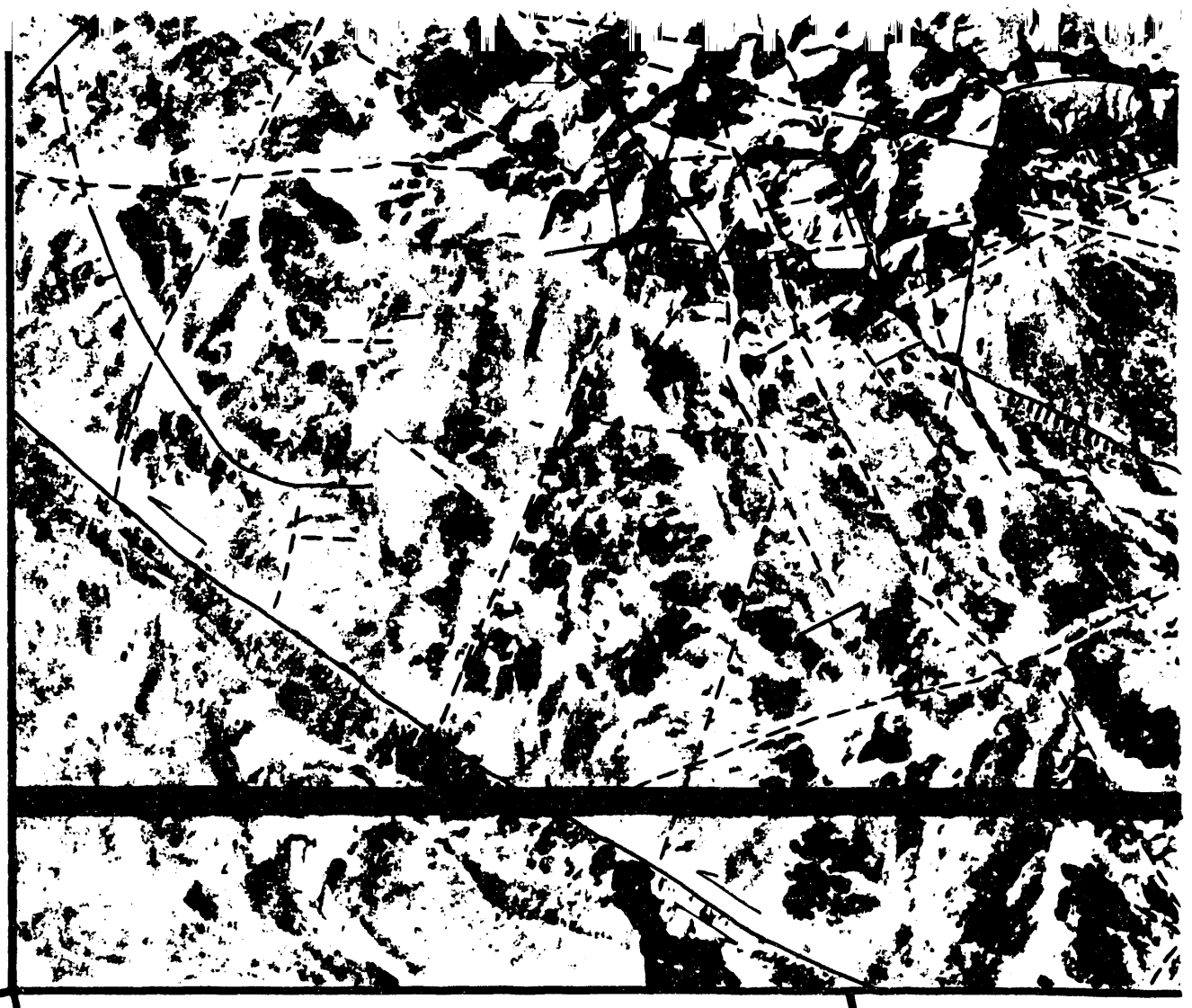

Base is Landsat Thematic Mapper band 4.

Structural geology mapped using Landsat Thematic Mapper filtered and false-color image products.

8° 00′E

ematic

ts.

MAP SHOWING THE STRUCTU

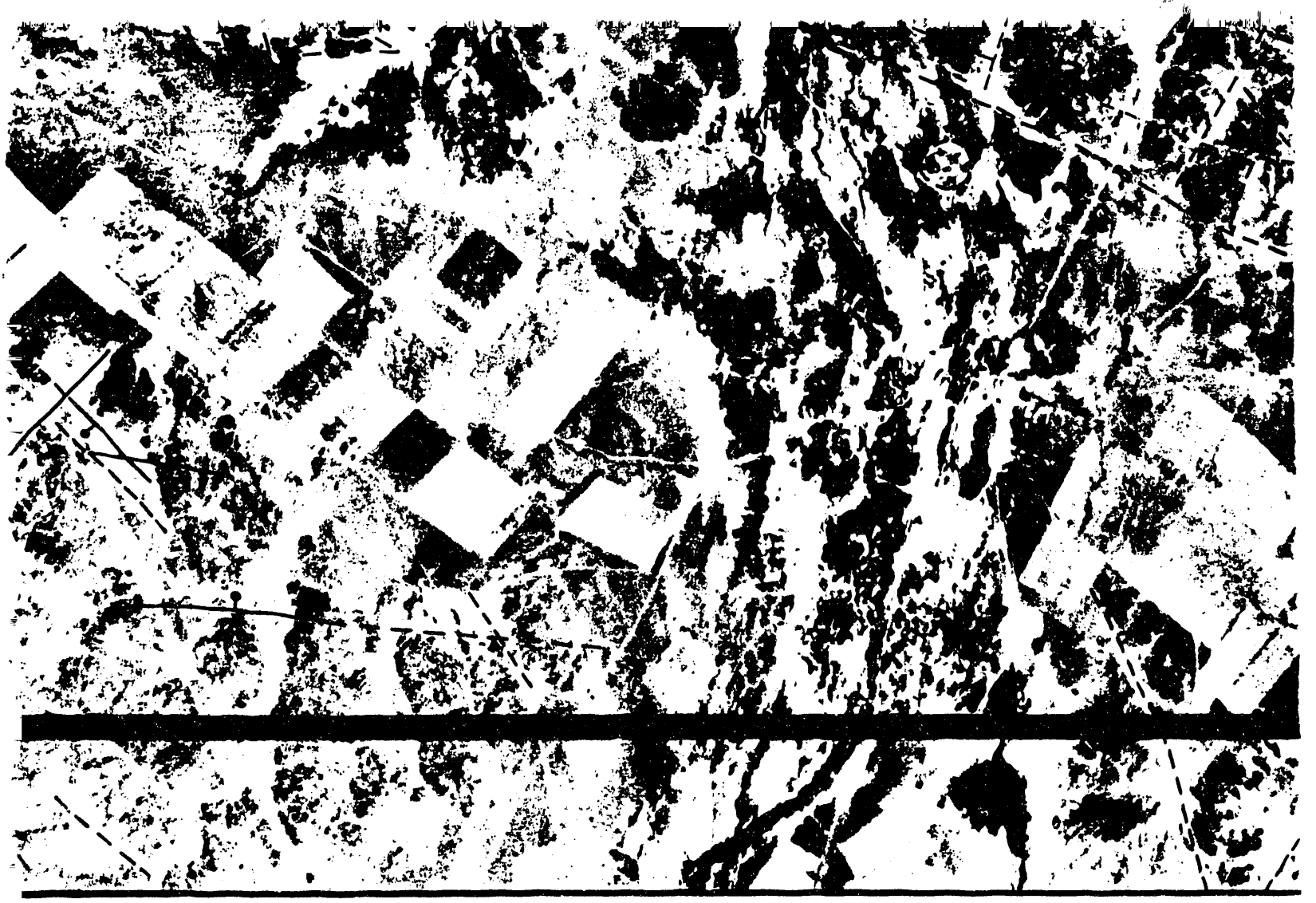

5 0 5 10 15 20

Scale 1:150,000

TURAL GEOLOGY IN THE SEMIPALATINSK

By

Gordon L. Dolin and Philip A. Davis

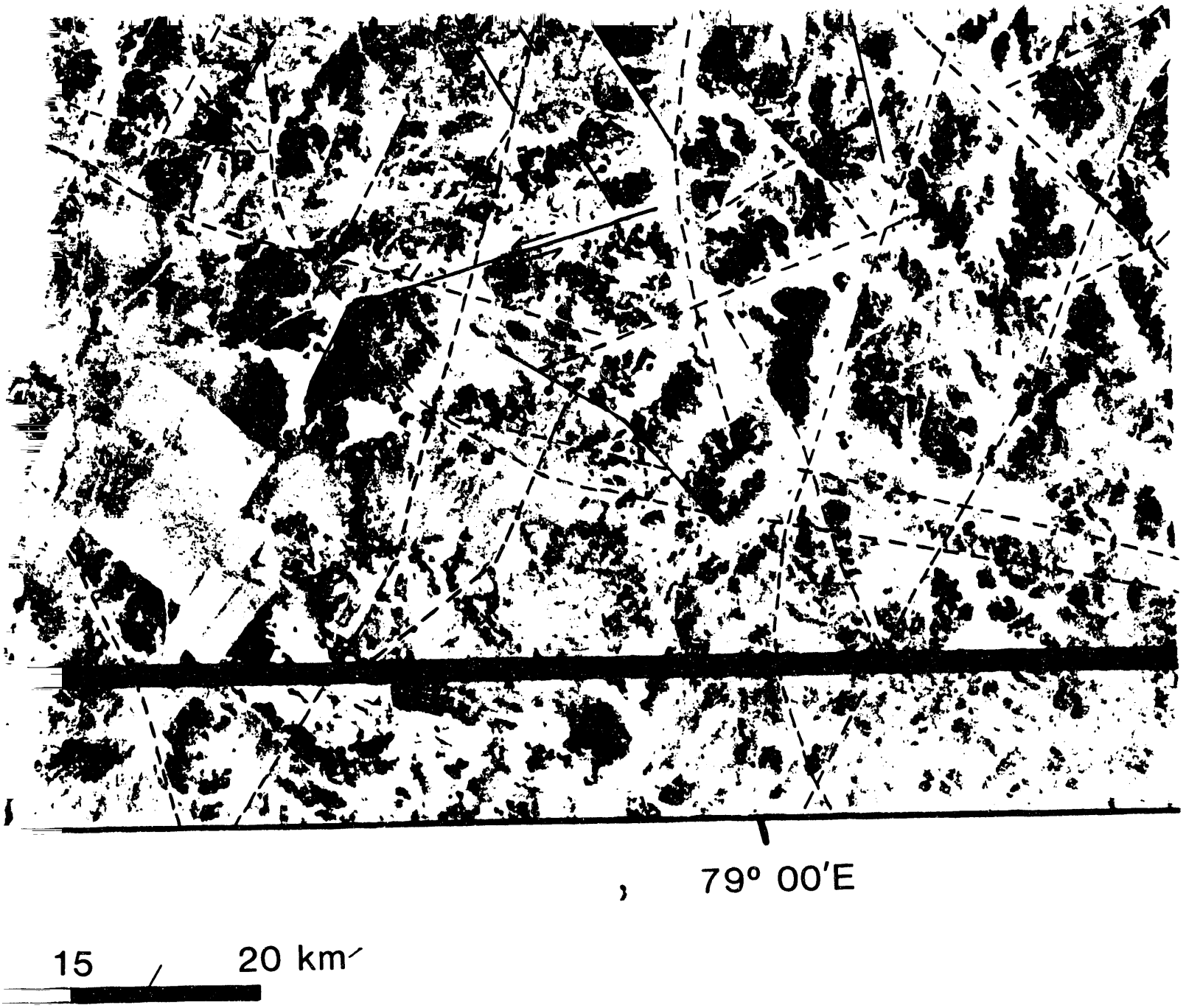

ALATINSK REGION, EASTERN KAZAKST

MAP SHOWING THE DRAINAGE FEATURES IN THE SEMIPALATINSK REGION, EASTERN KAZAKSTAN (SHEET 3 OF 3)

50° 22′44″N

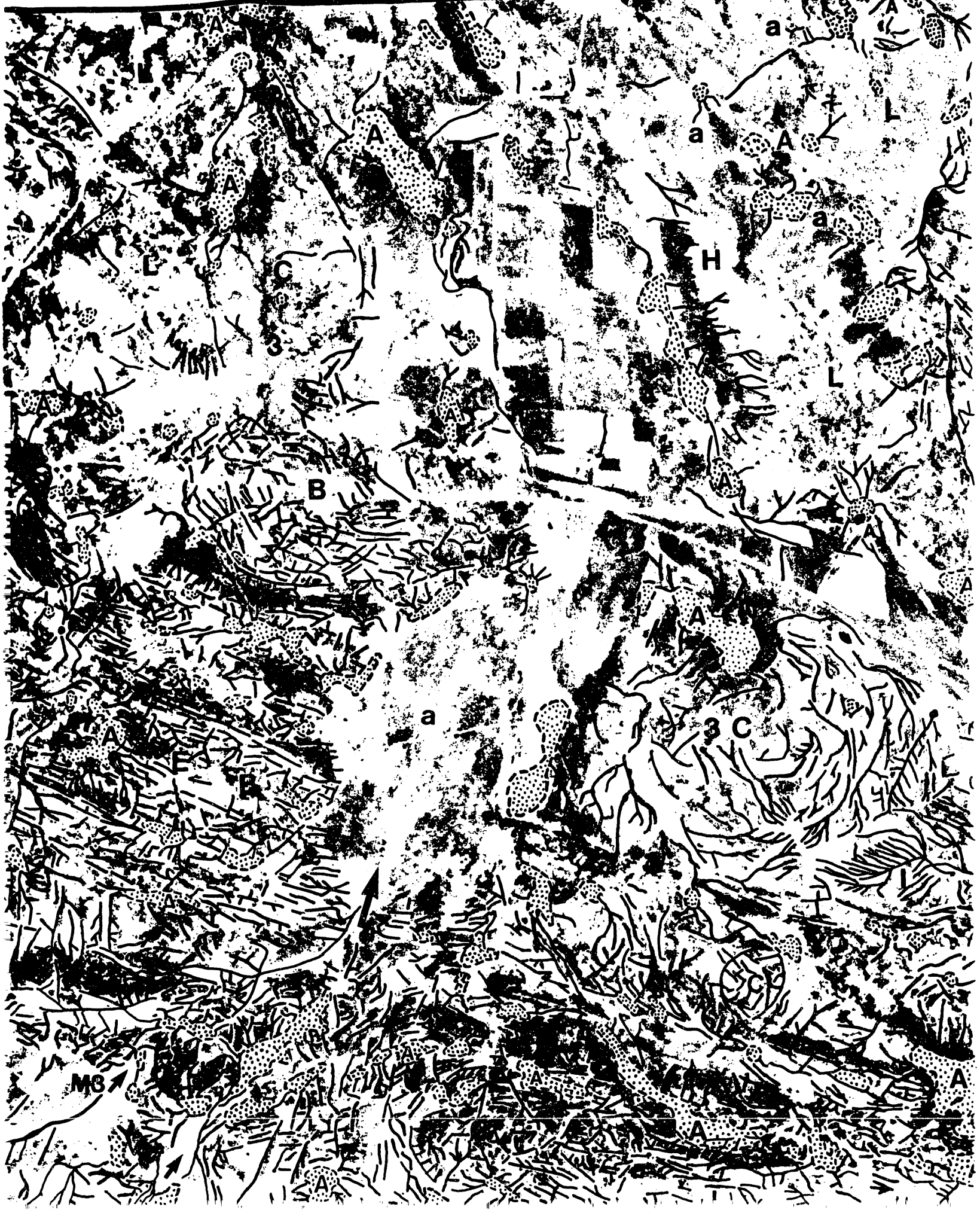
A
a
L
H
C
3
B
MB

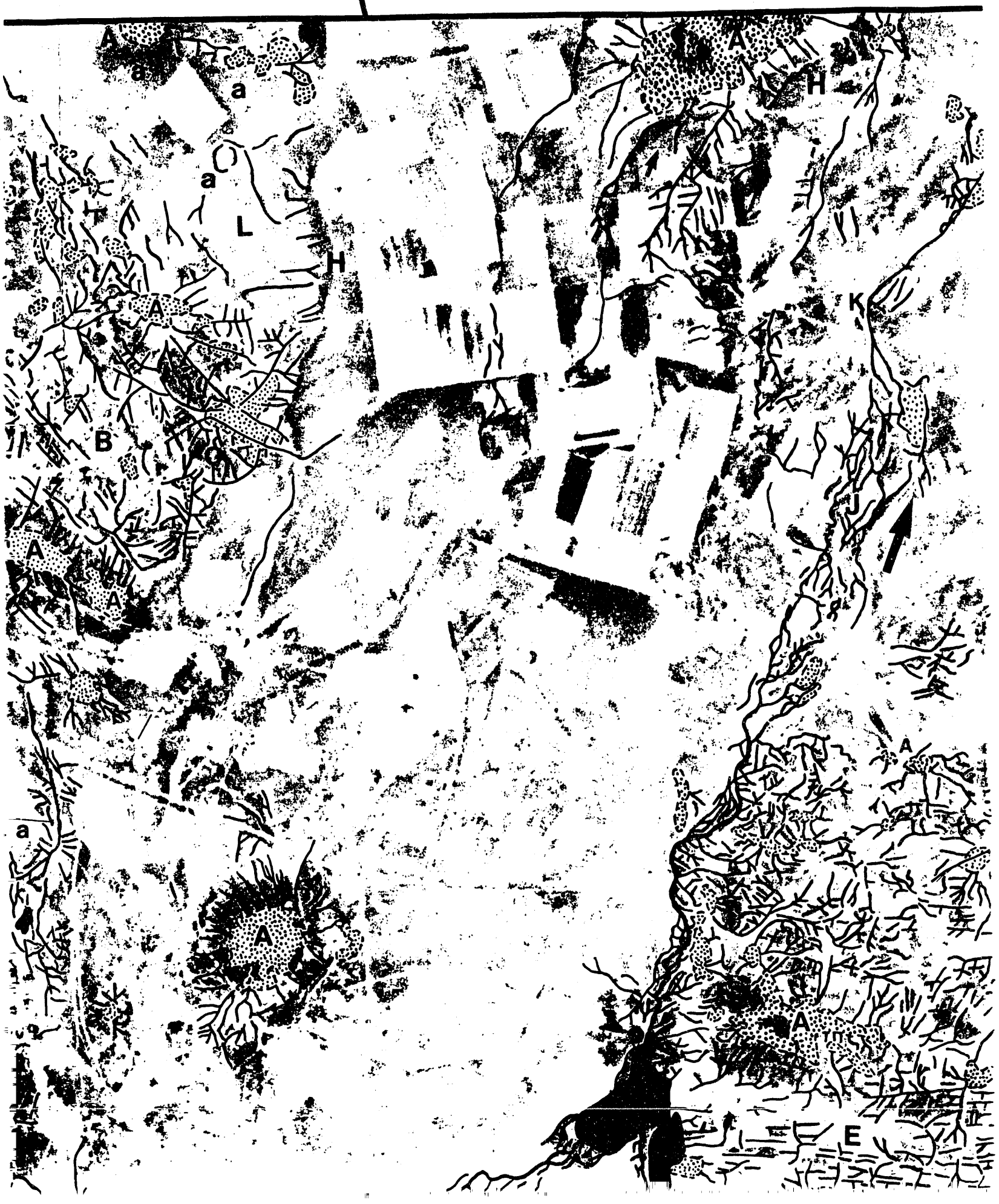
79° 00′E
A
a
a
a
L
H
A
B
A
A
a
A
A
H
K
J
A
A
E

J
M4
B
3
H
H
C
A
H
A
A
A
A
A
a
a
B
2
B
B
B
A

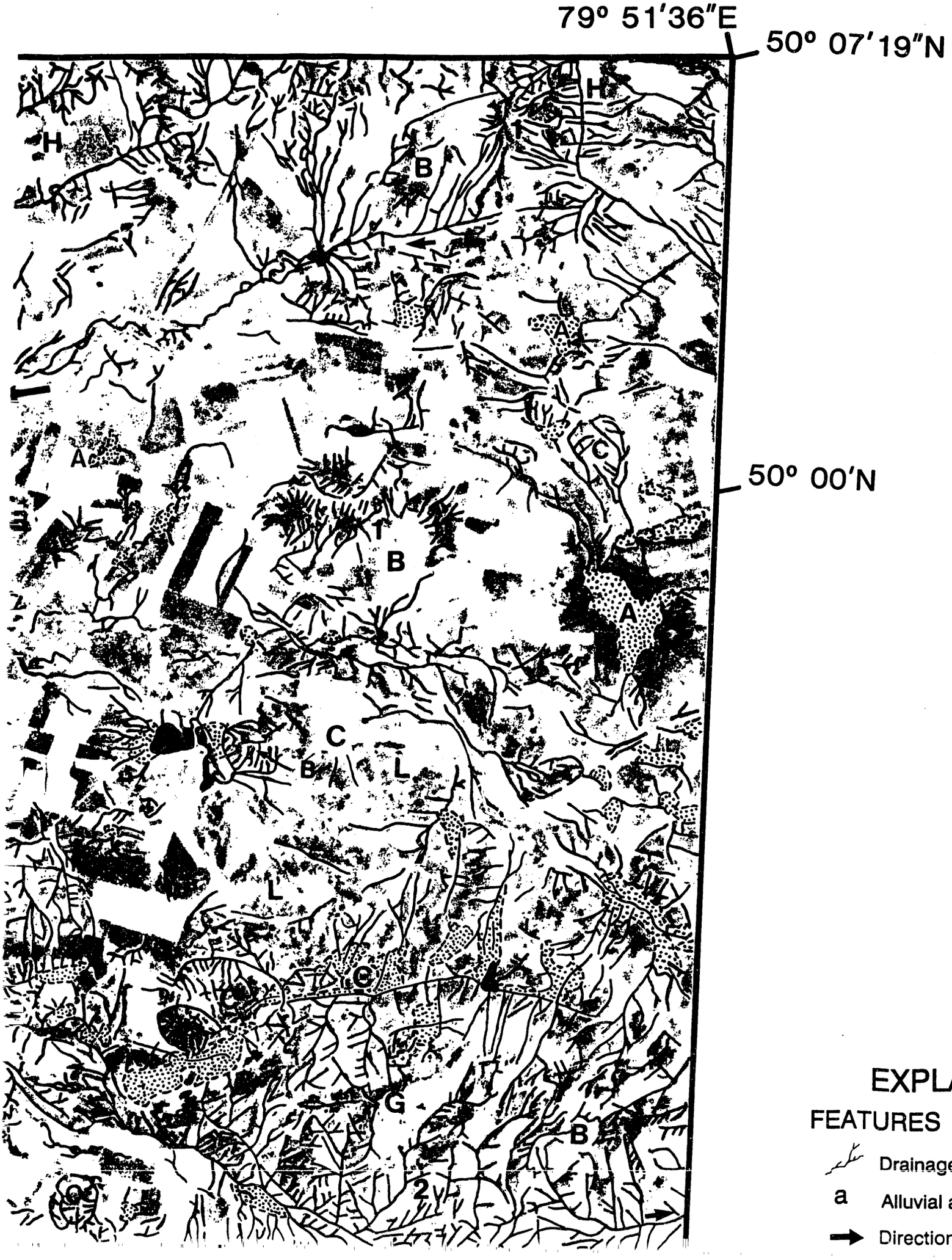
79° 51′36″E
50° 07′19″N
50° 00′N
H
H
B
A
A
C
T
B
A
C
B
L
L
C
G
B
2
MA
E
EXPLAN
FEATURES
Drainage co
a
Alluvial aprc
Direction of

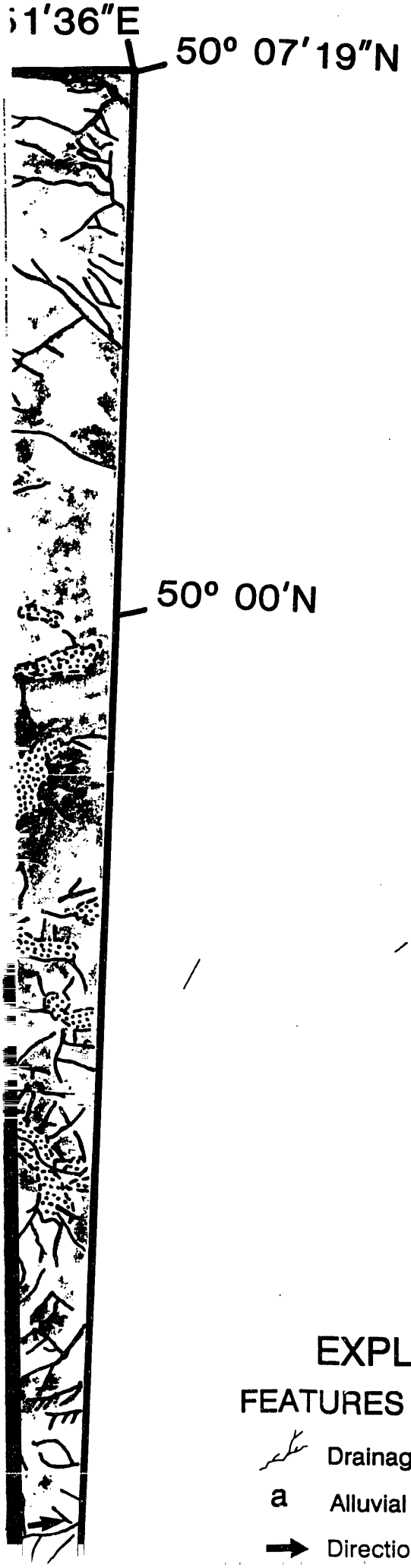

MAP SHOWING THE DRAINAGE FEATURES IN THE SEMIPALATINSK REGION, EASTERN KAZAKSTAN (SHEET 3 OF 3)

EXPLANATION

FEATURES

Drainage course

a Alluvial apron devoid of distinct channels

Direction of flow

50° 00′N

A
K
H
F
a
B
C

M1
E
a
a
a
A
M4
L
L
B
a
3
D
D
F
M3
A
3
D
B
A

E
B
B
a
C
M3
a
M3
M4
F
2
B
D
B
H
a
D
2
3
A
B
a

c. A.

Dir

St

Pl

DRAINA

A Ra

B Ra

C Ar

D De

E Mo

F Di

G Ar

H Pa

I As

J Br

K Co

L Int

M Ar

DRAINA

1 Fi

2 Me

3 Co

Direction of flow

Standing body of water

Playa or high-albedo alluvial deposit

DRAINAGE PATTERNS

A Radial, Centrpetal

B Radial, Centrifugal

C Annular

D Dendritic

E Modified Trellis

F Dichotomic

G Angulate

H Parallel

I Asymmetrical

J Braided

K Contorted

L Internal

M Anomalous (subcategories described in text)

DRAINAGE TEXTURES

1 Fine

2 Medium

3 Coarse

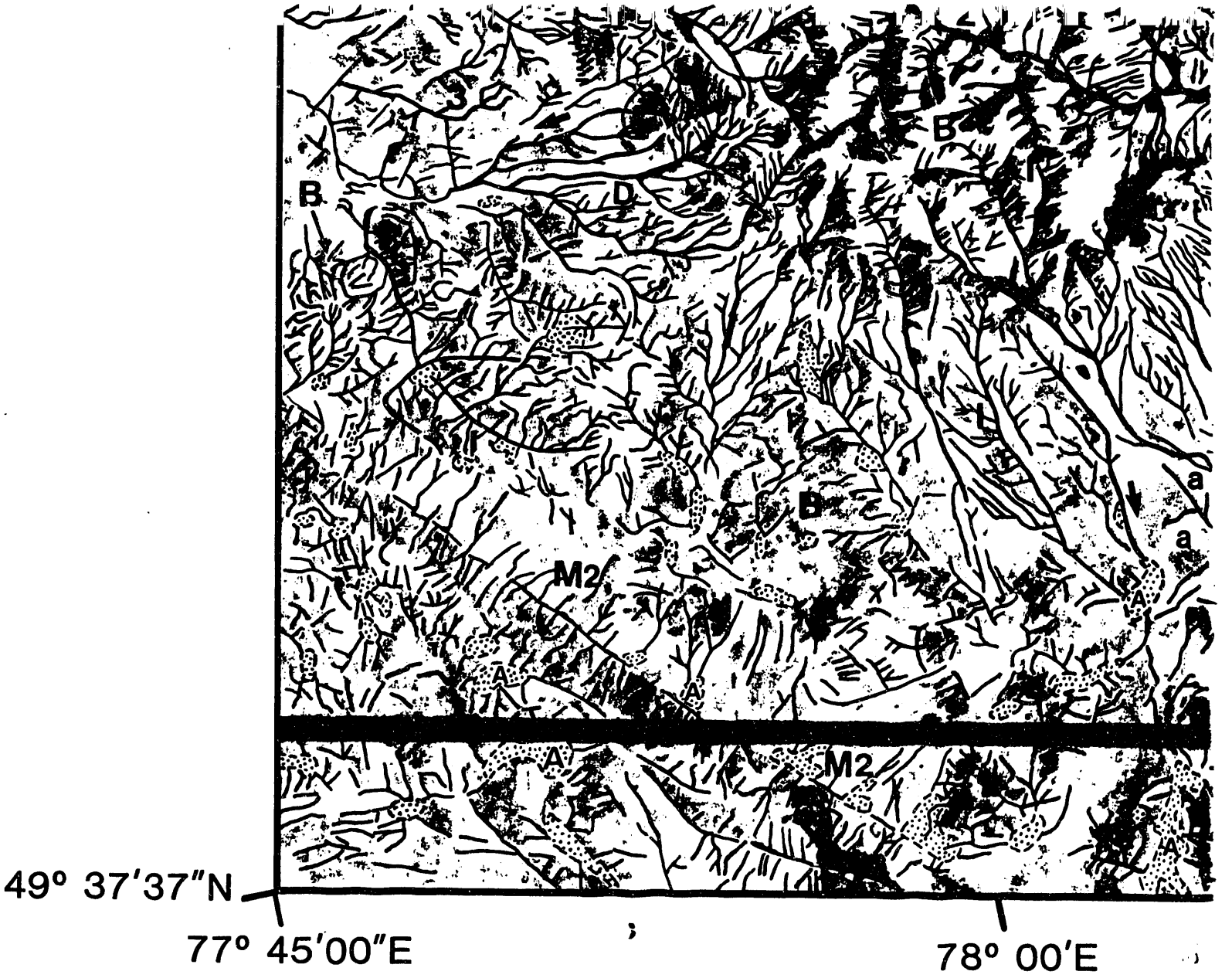

Base is Landsat Thematic Mapper band 4.

Drainage was mapped using Landsat Thematic Mapper filtered and false-color image products.

5 0

MAP SHOWING THE DRAINAGE FEATURES

5 0 5 10 15 20 km

Scale 1:150,000

E FEATURES IN THE SEMIPALATINSK REG

By

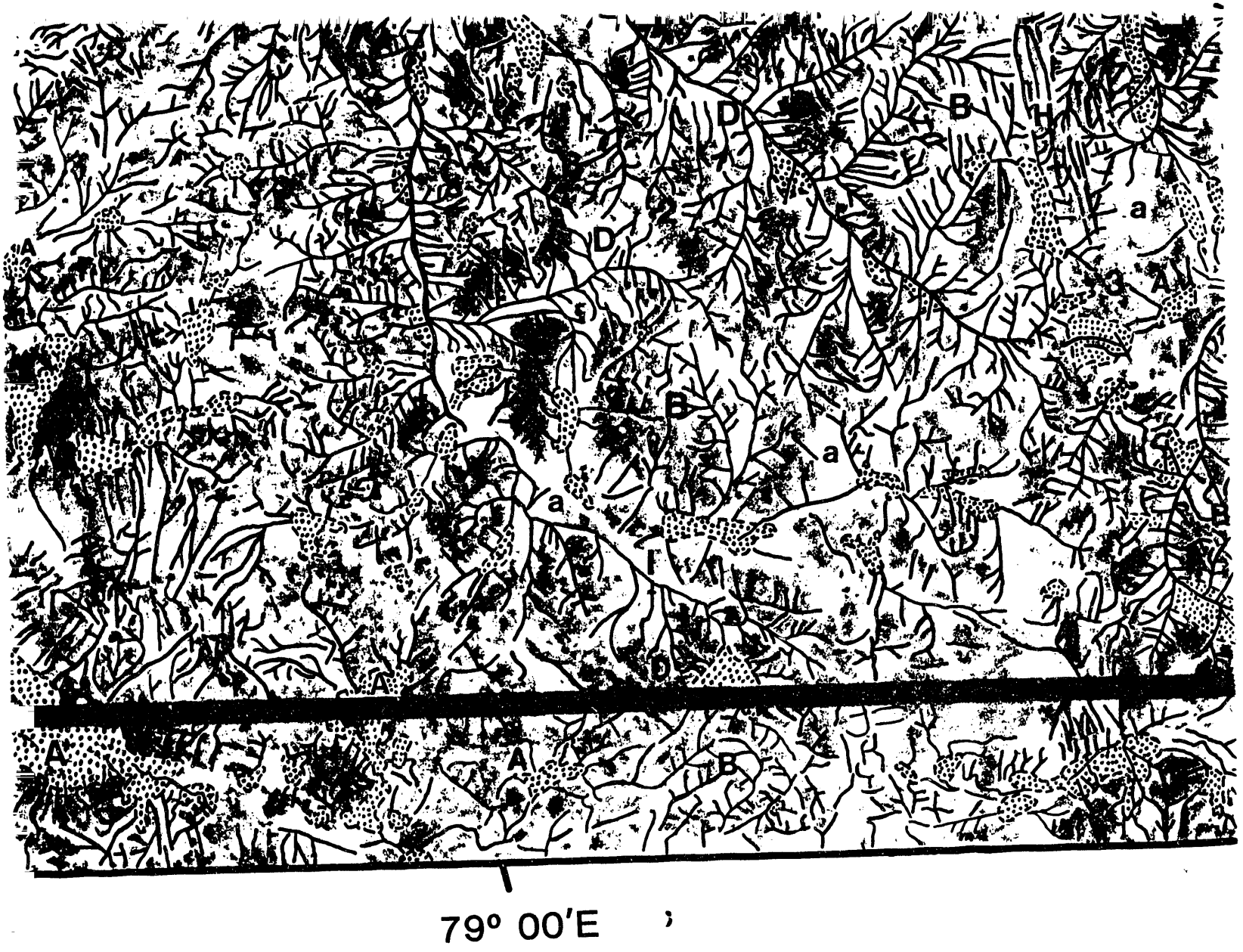

79° 00′E

km

REGION, EASTERN KAZAKSTAN

H
a
3 A
H
A
A
a
a
49° 22′48
79° 32′46″E

2 Medium

3 Coarse

49° 22′48″N

′46″E

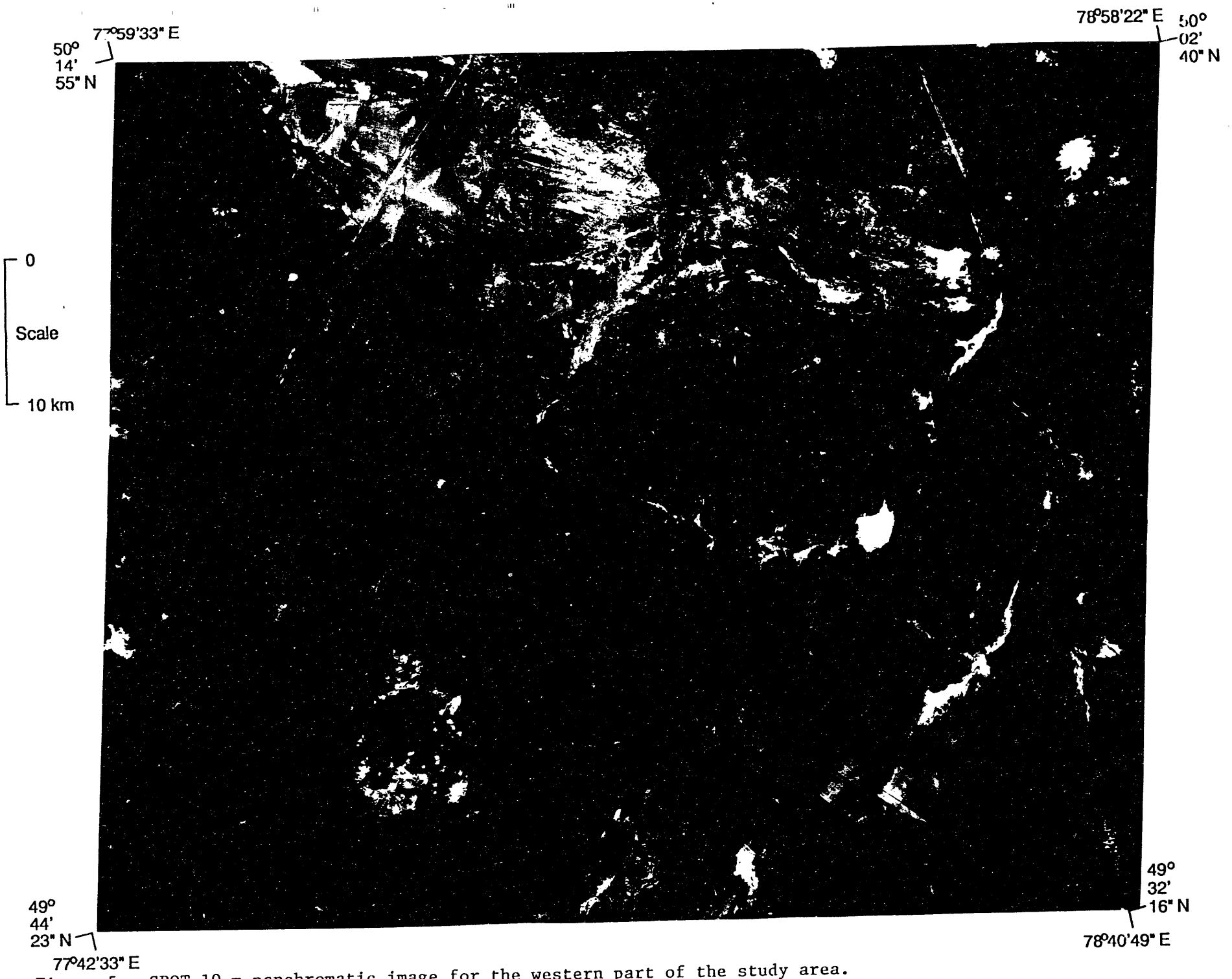

Figure 5. SPOT 10-m panchromatic image for the western part of the study area.

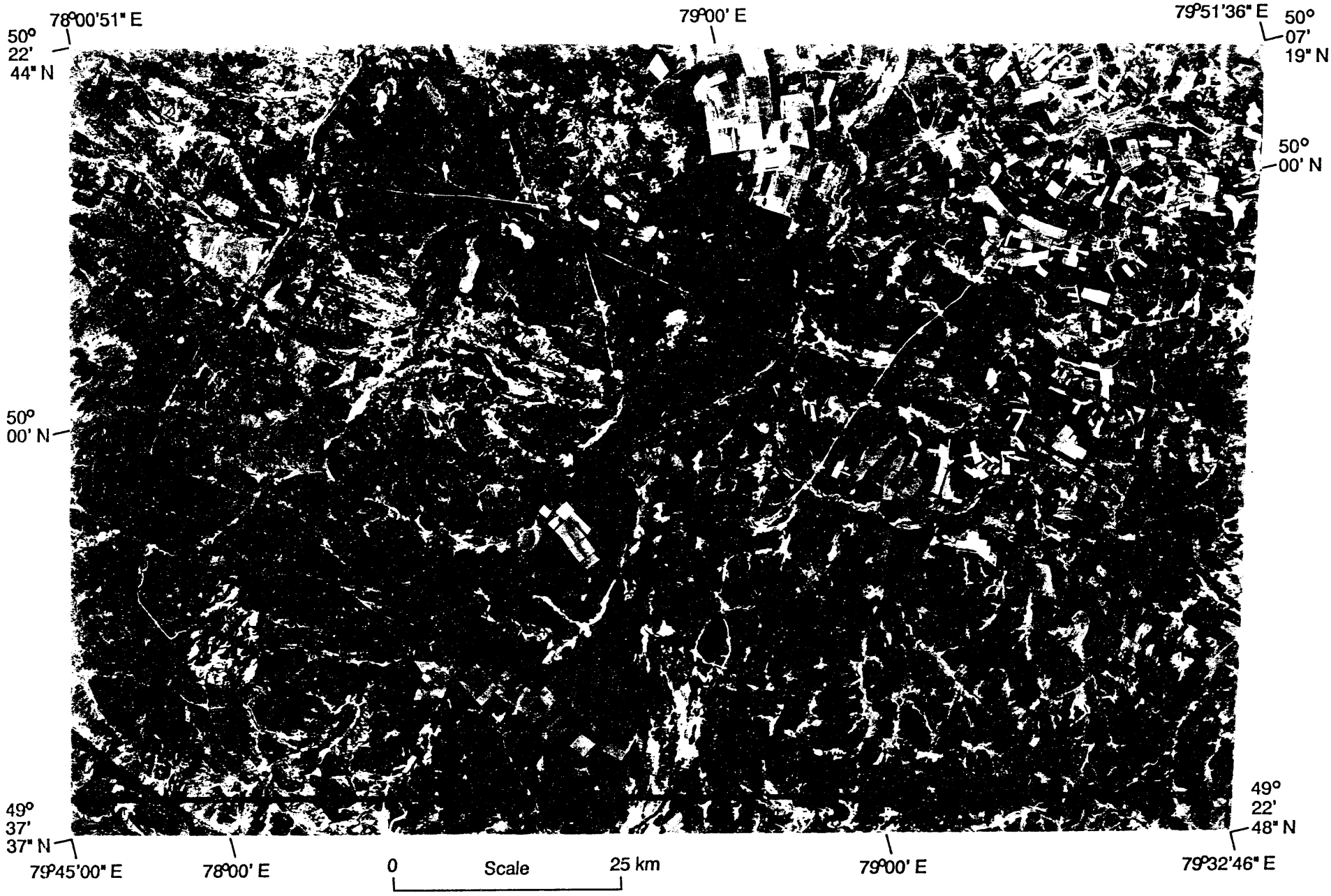

Figure 6. TM-band color-composite (BCC) image of the Semipalatinsk study area; TM band 1 displayed as blue, 4 as green, and 7 as red. We applied to each band's data a 101 X 101 pixel high-pass filter with 60% addback of each band's original data.

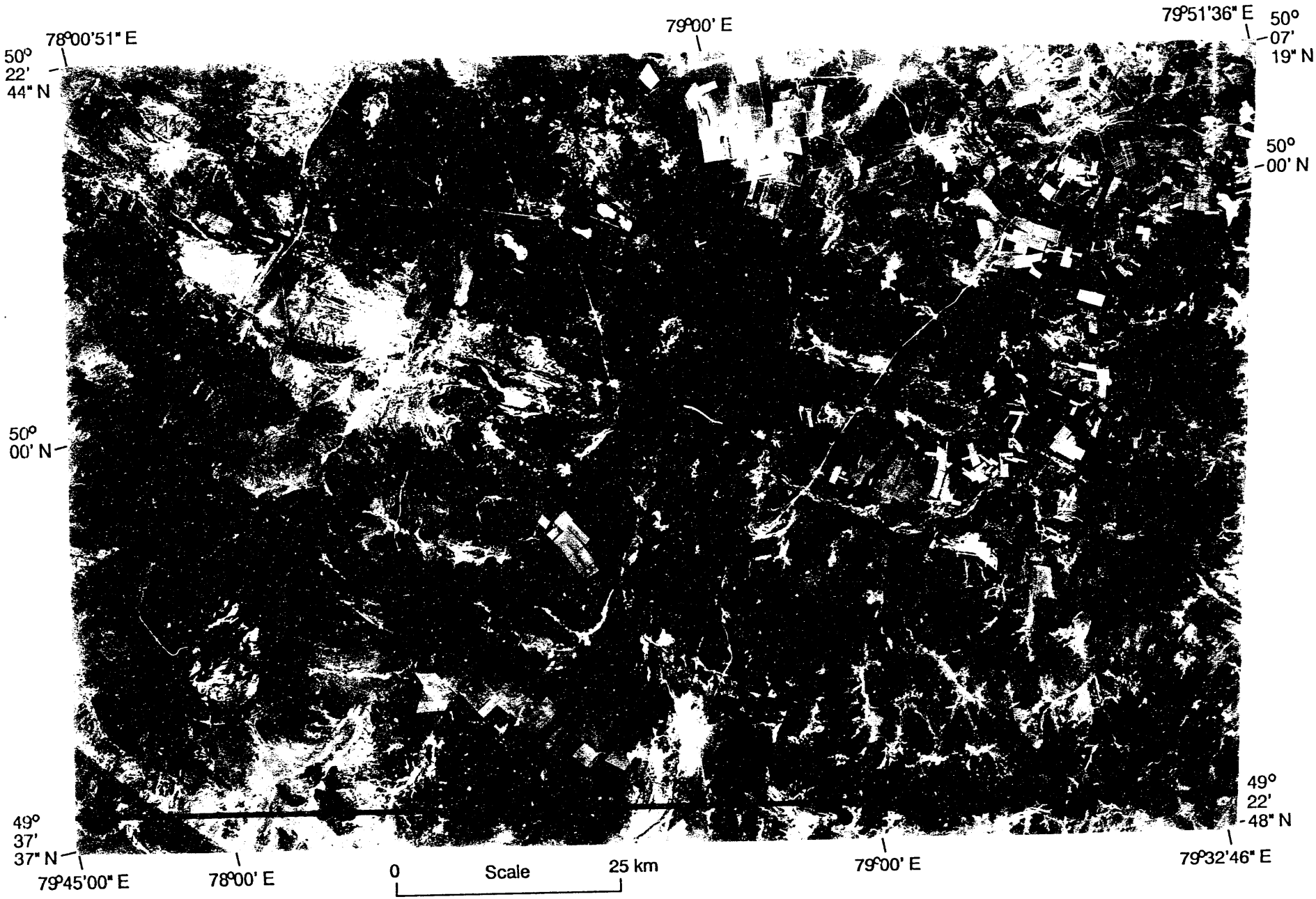

Figure 7. TM decorrelation-stretch color-composite (DSC) image of the Semipalatinsk study area resulting from principal-component analysis of TM bands 1, 4, and 7. The modified TM band 1 is displayed as blue, 4 as green, and 7 as red.

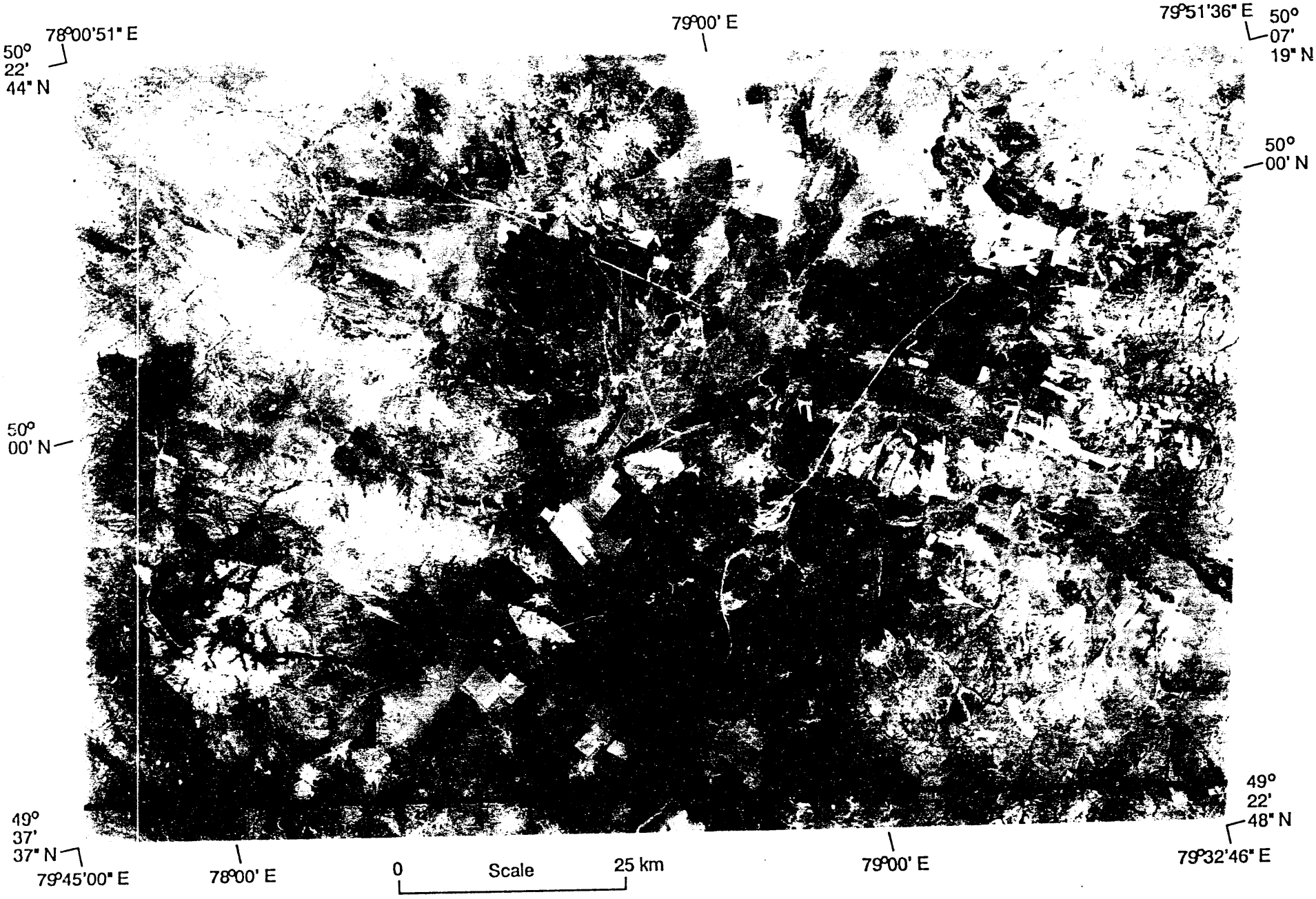

Figure 8. TM principal-component color-composite (PCC) image of the Semipalatinsk study area resulting from principal-component analysis on all six nonthermal Landsat TM bands. Principal component 1 is displayed as blue, component 4 as green, and component 5 as red.

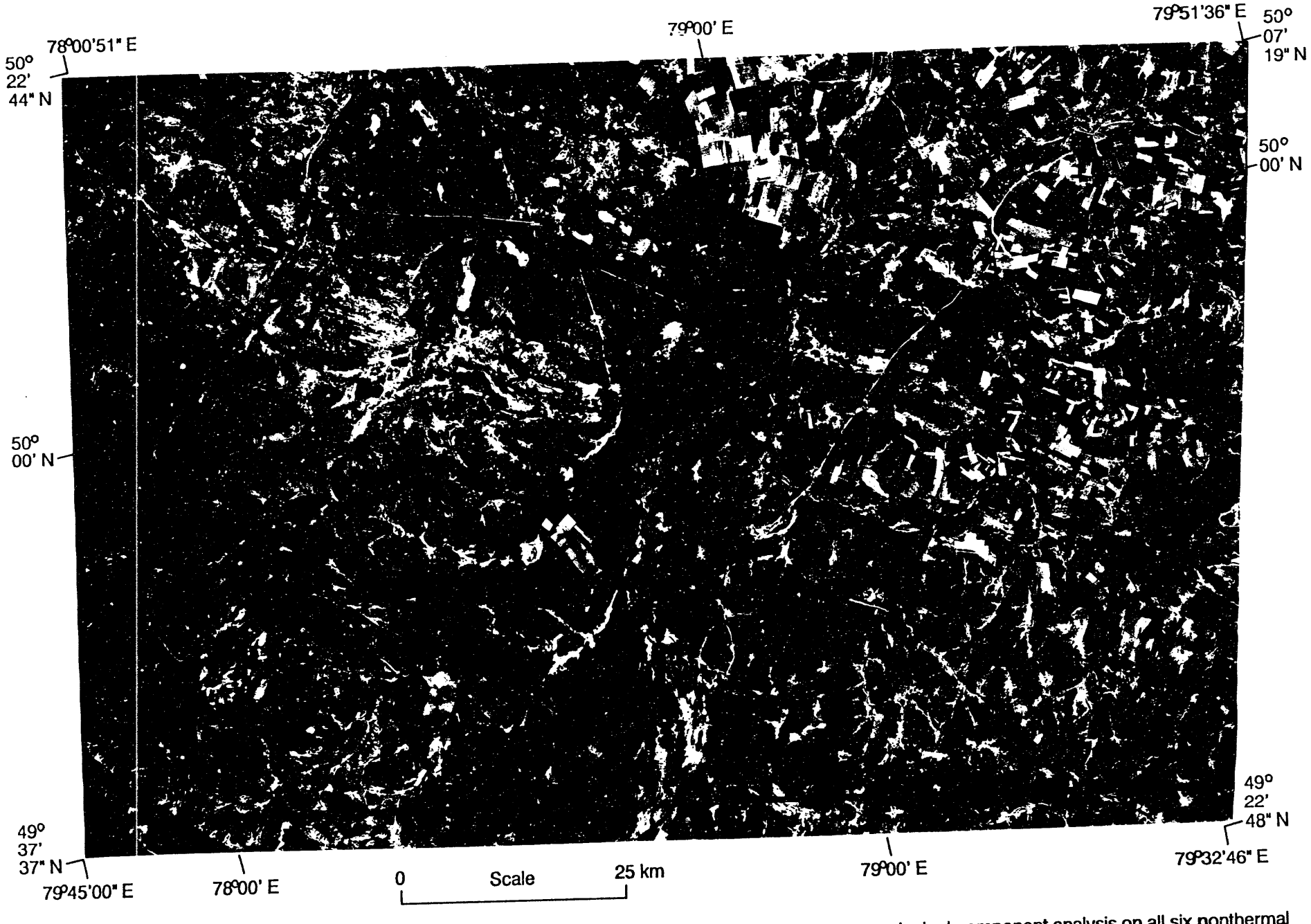

Figure 9. 101 X 101 pixel high-pass filtered (HPF) image of the first principal component that resulted from principal-component analysis on all six nonthermal Landsat TM bands.

LEGEND FOR GEOLOGIC MAP SHOWN IN FIGURE 10

GEOLOGIC UNITS

River deposits

Quaternary continental deposits

Gabbro (single dark-green unit in upper right corner)

Granite

Granodiorite

Tuff and lava (rhyolitic - dacitic)

Tuff and lava (andesitic - dacitic)

Tuff and lava (andesitic - basaltic)

Sedimentary rock (Cambrian - Cretaceous age); lithology not described; colors and patterns distinguish only ages

LINE SYMBOLS

River

Intermittent steam or wadi

Fault

Road

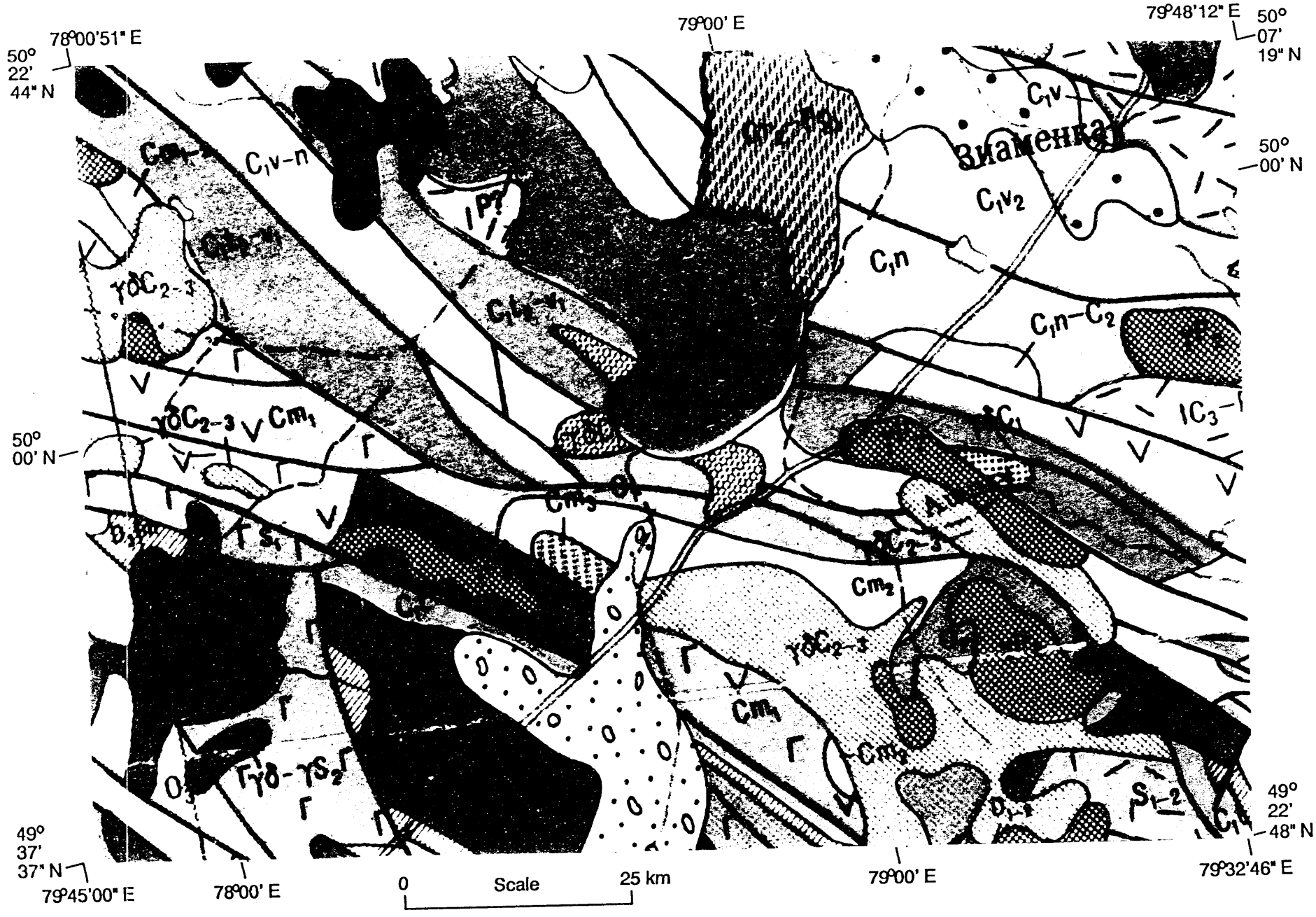

Figure 10. Portion of the largest-scale published geologic map that contains the Semipalatinsk study area (taken from Borovikov, 1972).

END

DATE
FILMED
12 / 1 / 93